# Trade-offs in muscle physiology in selectively bred High Runner mice

Alberto A. Castro, Theodore Garland, Jr., Saad Ahmed, Natalie C. Holt*

Department of Evolution, Ecology, and Organismal Biology, University of California, Riverside, Riverside, California 92521, USA

* To whom proofs, correspondence, and reprint requests should be addressed.

Telephone: (951) 827-2437

E-mail: natalieh@ucr.edu

Running title: Muscle trade-offs in High Runner mice

Key Words: Artificial selection, Endurance, Force-velocity, Locomotion, Muscle physiology, Trade-offs

## *Summary Statement*

We demonstrate a muscle-level trade-off between speed and endurance across replicated lines of mice experimentally selected for high levels of voluntary wheel running. However, this trade-off does not appear to underpin a previously reported organismal-level trade-off.

# *Abstract*

A trade-off between locomotor speed and endurance occurs in various taxa, and is thought to be underpinned by a muscle-level trade off. Among four replicate High Runner (HR) lines of mice, selectively bred for voluntary wheel-running behavior, a negative correlation between average running speed and time spent running has evolved. We hypothesize that this trade-off is due to changes in muscle physiology. We studied the HR lines at generation 90, at which time one line (L3) is fixed for the mini-muscle phenotype, another is polymorphic (L6), and the others (L7, L8) lack mini-muscle individuals. We used *in situ* preparations to quantify the contractile properties of the triceps surae muscle complex. Maximal shortening velocity varied significantly, being lowest in mini-muscle mice (L3 Mini=25.2, L6 Mini=25.5 mm $s^{-1}$), highest in normal-muscle mice L6 and L8 (40.4 and 50.3 mm $s^{-1}$ respectively), and intermediate in normal-muscle L7 mice (37.2 mm $s^{-1}$). Endurance, measured both as the slope of the decline in force and the proportion of initial force that could be sustained, also varied significantly. The slope was shallowest in mini-muscle mice (L3 Mini=-0.00348, L6 Mini=-0.00238), steepest in lines L6 and L8 (-0.01676 and -0.01853), and intermediate in L7 (-0.01145). Normalized sustained force was highest in mini-muscle mice (L3 Mini=0.98, L6 Mini =0.92) and lowest in L8 (0.36). There were significant, negative correlations between velocity and endurance metrics, indicating a muscle level trade-off. However, this muscle-level trade-off does not seem to underpin the organismal-level speed and endurance trade-off previously reported as the ordering of the lines is reversed; the lines that run the fastest for the least time have the lowest muscle complex velocity and highest endurance.

# *Introduction*

Trade-offs, limits to adaptation, and multiple solutions have long been held as cornerstones in evolutionary biology, and in many sub-fields of organismal biology (Garland & Carter, 1994; Ackerly *et al.*, 2000; Martin *et al.*, 2015; Agrawal, 2020). Multiple types of trade-offs have been recognized (Cohen *et al.*, 2020; Mauro & Ghalambor, 2020; Garland *et al.*, 2022). Perhaps the most common type involves allocation constraints. For example, if the energy available to an organism is limited, then spending more on one function (e.g., disease resistance) means less is available for other functions (e.g., reproduction). A different type of trade-off occurs when features that enhance performance of one task decrease performance of another (Garland *et al.*, 2022). Such functional conflicts are apparent in bone and muscle biomechanics, for example, the relative lengths of in-levers and out-levers in the skeletal system (Santana, 2016), and force-velocity trade-offs in muscle (Herrel *et al.*, 2009; Schaeffer & Lindstedt, 2013).

In the locomotor system, the most commonly studied potential trade-off at the level of organismal performance is the sometimes-negative relationship between speed and endurance. For example, among 12 species of closely related lacertid lizards, speed and endurance capabilities are negatively related after accounting for variation in body size (Vanhooydonck *et al.*, 2001). However, this trade-off is not apparent among species of phrynosomatid lizards (Albuquerque *et al.*, 2015; see also Toro *et al.*, 2004; Goodman *et al.*, 2007). Many studies have also tested for trade-offs at the level of variation among individuals. For example, statistically significant trade-offs were detected between speed-related and endurance-related events in a study of 1,369 elite human athletes participating in heptathlon and decathlon events (Careau & Wilson, 2017), and between terrestrial exertion capacity and aquatic burst performance in male tropical clawed frogs (*Xenopus tropicalis*) (Herrel & Bonneaud, 2012). When present, the

84 organismal-level trade-off between speed and endurance is thought to be underpinned by a
85 muscle-level trade off, presumably caused by the co-variation of myosin isoform expression and
86 oxidative capacities across muscle fibers (e.g., see Garland, 1988).
87 Mammalian muscle fiber types vary along a continuum of contractile and metabolic
88 properties (for a review see Schiaffino & Reggiani, 2011). At one end of the spectrum, Type I
89 fibers contract slowly, use oxidative metabolism, have low power outputs, and are fatigue
90 resistant. At the other end, Type IIb fibers contract rapidly, use glycolysis, have high power
91 outputs, and fatigue rapidly. Type IIa fibers are intermediate, being fast-twitch, more fatigue
92 resistant than Type IIb fibers, and using both oxidative and glycolytic metabolisms (Komi, 1984;
93 Gleeson & Harrison, 1988; Rome *et al.*, 1988; Esbjörnsson *et al.*, 1993; Schiaffino & Reggiani,
94 2011). Muscle fiber type variation has clear links with locomotor diversity. For instance, the
95 predominance of Type I fibers in the forelimb muscles of slow-moving sloths (Spainhower *et al.*,
96 2018) contrasts with the predominance of Type IIb fibers in the hindlimb muscles of fast-
97 sprinting cheetahs (Williams *et al.*, 1997). The variation in locomotor performance among lizard
98 species also seems to relate to variation in muscle fiber types (Bonine *et al.*, 2005;
99 Vanhooydonck *et al.*, 2014; Albuquerque *et al.*, 2015; Scales & Butler, 2016).
100 Selection experiments and experimental evolutionary approaches (Garland & Rose, 2009)
101 present unique opportunities to study mechanisms underlying trade-offs (discussed in Garland *et*
102 *al.*, 2022). In the present study, we use 4 replicate lines (lab designated as lines 3, 6, 7 and 8,
103 henceforth referred to as L3, L6, L7 and L8) of high runner (HR) mice to explore the muscular
104 basis of organismal-level trade-offs between speed and endurance. These HR mice have been
105 selectively bred for 90 generations based on the average number of wheel revolutions on days 5
106 & 6 of wheel access when young adults (Swallow *et al.*, 1998). The HR lines evolved rapidly

and reached selection limits after ~17-27 generations (Careau *et al.*, 2013), at which point mice from all 4 HR lines run approximately three-fold more than mice in the 4 non-selected Control (C) lines. HR mice also have increased endurance and maximal aerobic capacity ($VO_2$ max) during forced treadmill exercise, larger hearts, and larger brains, among various other phenotypic and genetic differences (Garland, 2003; Meek *et al.*, 2009; Kolb *et al.*, 2010, 2013; Hillis *et al*., 2020; Castro *et al*., 2022).

One striking discovery in the HR selection experiment was the "mini-muscle" phenotype, characterized by a 50% reduction in the mass of the triceps surae muscle complex (Garland *et al.*, 2002), caused primarily by a dramatic reduction in type IIb muscle fibers (Guderley *et al.*, 2006; Talmadge *et al.*, 2014). The gastrocnemius muscle was considerably lighter in mini-muscle individuals and *in vitro* studies of muscle properties showed some evidence of slower twitches, altered curvature of the force-velocity relationship, reduced power production, and improved endurance in this muscle (Syme *et al.*, 2005). In contrast, the soleus muscle was 30% larger in mini-muscle mice, and its contractile properties were largely unaltered, other than the observation of some faster twitch properties in one of the mini-muscle groups (Syme *et al.*, 2005). One of the HR lines (L3) became fixed for the mini-muscle phenotype sometime between generations 22 and 36 (Garland *et al.*, 2002; Syme *et al.*, 2005), while another line (L6) remains polymorphic after 95 generations (Hiramatsu *et al.*, 2017; Cadney *et al.*, 2021).

Across all 4 replicate HR lines, but not across the 4 Control lines, Garland *et al.* (2011) reported a significant negative correlation between average running speed (wheel revolutions per minute) and time spent running (minutes of wheel running per day) at generation 43. In the base population, these two traits were positively correlated both phenotypically and genetically (Swallow *et al.*, 1998), and we might expect that the evolution of an organismal speed and

endurance trade-off could be related to evolved changes in lower-level traits, specifically in skeletal muscle. Therefore, the purpose of the present study was to examine muscle contractile properties to determine whether a muscle-level trade-off underlies the negative relationship between the duration of daily running and the average running speed that has evolved across the replicate HR lines.

We quantified the speed and endurance properties of an important locomotor muscle group in mice, the triceps surae complex, which contains the fast medial gastrocnemius, lateral gastrocnemius, and plantaris muscles, along with the slow soleus muscle (Zhan *et al.*, 1999; Houle-Leroy *et al.*, 2003; Guderley *et al.*, 2006; McGillivray *et al.*, 2009; Schaeffer & Lindstedt, 2013; Talmadge *et al.*, 2014). We studied this entire muscle complex *in situ*, as opposed to studying individual muscles *in vitro*, as we believe this provides the best assessment of muscle speed and endurance in the context of locomotion. In future studies, it would also be of interest to examine the contractile properties of individual muscles.

In *in situ* preparations, the muscle complex remains connected to a functioning circulatory system. This avoids the complication of diffusion limitations (Barclay, 2005) during *in vitro* endurance tests, therefore allowing for more physiologically realistic measurements of muscle endurance. In addition to retaining a connection to the circulatory system, *in situ* study of the triceps surae muscle complex allows for simultaneous activation of all muscles within this complex, and determination of its emergent contractile properties. This simultaneous activation ignores physiological recruitment (Liddell and Sherrington 1925; Henneman *et al*., 1957; Morris and Askew, 2010; Holt *et al*., 2014), such as the increase in total activation of the triceps surae complex, and particularly that of faster fibers, with increasing speed and incline in running rats (Hodson-Tole and Wakeling, 2008). However, this phenomenon is also ignored *in vitro*

153 preparations in which muscles are typically maximally activated despite the variation in
154 activation that occurs within a single muscle across locomotor conditions (Hodson-Tole and
155 Wakeling, 2008; Morris and Askew, 2010). Perhaps more importantly than the somewhat
156 unrealistic activation patterns, this approach limits our ability to attribute aspects of performance
157 to individual muscles. However, locomotion is not powered by individual muscles, but rather
158 driven by torques around joints produced by synergistic muscles, such as the triceps surae
159 complex. Hence, the emergent properties of this muscle complex seem the most relevant to
160 locomotion. This is particularly important in the HR mice, as a previous comparison of just a
161 subset of HR lines showed that the mini-muscle phenotype has different effects on the various
162 muscles within the triceps surae muscle complex (Syme *et al*., 2005). Hence, examination of any
163 single muscle would likely not be reflective of the cumulative effects of selection.
164 This study uses an *in situ* triceps surae complex preparation to determine the isometric
165 twitch times and isotonic force-velocity properties as metrics of the speed of the muscle
166 complex, and the changes in force over hundreds of isometric tetanic contractions as metrics of
167 the endurance of the muscle complex. Although not entirely representative of muscle function
168 during locomotion, these metrics were chosen as they provide good estimates of the bounds of
169 muscle speed and endurance, and can be reliably measured in a multiple muscle preparation.
170 Based on the assumption that muscle properties at least partly underpin the organismal-
171 level trade-off between speed and endurance, we hypothesized that muscle complex speed and
172 endurance metrics would trade-off in HR lines in a way that parallels the documented organismal
173 variation in wheel-running speed and duration (Garland *et al.*, 2011). At the organismal level,
174 L8 mice ran for the longest and had the slowest mean wheel-running speeds (Garland *et al.*,
175 2011), while L3 mice had the fastest mean speeds on wheels and ran for the shortest total

duration. Hence, we hypothesized that muscle complexes from L8 mice would have the highest endurance and the lowest velocity, while muscle complexes from L3 mice would be the opposite. However, these predictions seem to at odds with the findings of Syme *et al*. (2005) mentioned previously, who found L3 and L6 mini-muscle mice to generally have slower, more fatigue-resistant, medial gastrocnemius muscles, with only marginal evidence for faster soleus muscles in L6 mini-muscle mice.

In contrast to Syme *et al* (2005), we compare muscle properties across all 4 replicate lines of HR mice, and examine the speed and endurance properties of the entire triceps surae complex. This allows us to compare any trade-offs in muscle complex properties to the organismal-level trade-offs reported across all HR lines ~10 generations after Syme *et al.* (2005). Moreover, we can use the knowledge gained from this prior study of a subset of HR lines (Syme *et al.,* 2005), namely that the properties of individual muscles vary differently across lines, to inform the design of this study in which we examine the emergent properties of the entire triceps surae complex. We believe this provides novel insight into the muscle-level determinants of organismal performance with particular reference to the role of the trade-off between speed and endurance in the evolution of locomotor performance.

# *Materials and Methods*

## The High Runner Mouse Model

Mice from the 4 High Runner (HR) lines are bred for voluntary wheel running during 6 days of wheel access as young adults, and are compared with 4 non-selected Control (C) lines (Swallow *et al.*, 1998). Briefly, the founding population was 224 laboratory house mice (*Mus*

198 *domesticus*) of the outbred, genetically variable Hsd:ICR strain (Harlan-Sprague-Dawley,
199 Indianapolis, Indiana, USA). Mice were randomly bred for two generations and then separated
200 into 8 closed lines, which consist of 10 breeding pairs each generation. During the routine
201 selection protocol, mice are weaned at 21 days of age and housed in groups of 4 individuals of
202 the same sex until ~6-8 weeks of age. Mice are then housed individually in cages attached to
203 computer-monitored wheels (1.12 m circumference, 35.7 cm diameter, and 10 cm wide wire-
204 mesh running surface) with a recording sensor that counts wheel revolutions in 1-min intervals
205 over 6 days of wheel access (Swallow *et al.*, 1998; Careau *et al.*, 2013; Hiramatsu, 2017). In the
206 HR lines, the highest-running male and female from each family are chosen as breeders. The
207 selection criterion is total wheel revolutions on days 5 and 6 to avoid potential effects of
208 neophobia during the initial exposure to wheels. Sibling mating is not allowed. Mice are kept at
209 room temperatures of approximately 22°C, with ad lib access to food and water and a 12L:12D
210 photoperiod.
211

212 # Study Animals

213 To examine whether trade-offs in muscle properties underlie the trade-off between
214 average running speed and duration that has evolved among the HR lines (Garland *et al.*, 2011),
215 we studied all four of the HR lines (L3, L6, L7, and L8). Female mice (N = 31) from generation
216 90 of the selection experiment were housed 4/cage beginning at weaning. We chose HR females
217 because they generally run greater daily distances, at higher average speeds, than HR males
218 (Garland *et al.*, 2011), thus making it more likely that muscle-based trade-offs might be relevant.
219 As noted in the Introduction, the "mini-muscle" phenotype presently occurs in a subset of
220 the HR mice. In our sample of 31 mice (not all of which had data for all traits), the number of

mini-muscle individuals was all of 6 in L3 and 5 of 11 in L6. The presence of the mini-muscle phenotype means that rather than 4 lines, we instead have five total groups: L3 Mini (N=6), L6 Mini (N=5), L6 (N=6), L7 (N=8), and L8 (N=6). Based on previous studies (Syme et al., 2005), we expected that these sample sizes will provide sufficient power to demonstrate any differences between groups.

All mice were housed at room temperature with food and water ad libitum. All experiments were approved by the University of California, Riverside Institutional Animal Care and Use Committee. Given the time it takes to perform surgical experiments on individuals from all 4 replicate lines of HR mice, the use of mice from a single generation, and because of breeding constrains due to nature of the HR mouse selection experiment (see Swallow *et al.*, 1998), there was some necessary variation in age. Mice ranged from 46-107 days old. To account for this variation, age was included as a covariate in all analyses.

## Surgical Procedure

The twitch, tetanic, force-velocity, and endurance properties of the left triceps surae muscle group, were determined *in situ*. Mice were anaesthetized (SomnoSuite Low-flow Anesthesia System, Kent Scientific, Torrington, CT, USA) and maintained at 1.5-5% isoflurane anesthesia. The depth of anesthesia was continually monitored, and the dosage adjusted to maintain a sufficient depth. Body temperature was monitored using a thermometer inserted into the rectum, and maintained throughout surgery *via* an integrated system that continuously adjusted the temperature of the heat pad placed under the animal (RightTemp System, Kent Scientific, Torrington, CT, USA). The sciatic nerve was surgically exposed, and a bipolar nerve cuff for electrical stimulation of the triceps surae complex was placed around it. Mineral oil was

applied at the attachment site to keep the nerve moist, and the incision was closed. The proximal end of femur was exposed and clamped into a custom-made stereotaxic frame. The Achilles tendon was exposed distally, Kevlar thread tied tightly around it, and the calcaneus cut. The end of the free tendon was attached to the lever arm of a servomotor (305C-LR Dual-Mode Lever System, Aurora Scientific, Aurora, ON, CA), allowing for measurements of muscle force, length, and velocity in the triceps surae complex (Ranatunga, 1984; Claflin & Faulkner, 1989; Zhan *et al.*, 1999; Syme *et al.*, 2005; Holt *et al.*, 2016; Javidi *et al.*, 2020).

## Muscle Activation and Data logging

All recordings and data processing were performed using data acquisition software (IgorPro 7, WaveMetrics, Lake Oswego, OR, USA). Stimulation protocols were sent to the muscle, and data logged, at a sampling frequency of 10,000 HZ using a DAQ AD board (CompactDAQ, National Instruments, Austin, TX, USA). Supramaximal square wave pulses (amplitude 1-2 mA, pulse duration 0.1 ms) were constructed (IgorPro 7, WaveMetric, Lake Oswego, OR, USA) and applied to the sciatic nerve (CompactDAQ, National Instruments, Austin, TX, USA; High-Power, Biphase Stimulator, Aurora Scientific, Aurora, ON, CA) (Holt & Azizi, 2014). The brief pulse duration (0.1 ms) required to prevent damage to the sciatic nerve necessitated the high frequency sampling used (10,000 Hz). Single pulses were used to elicit all twitch contractions, while 350 ms trains of pulses delivered at 80 Hz were used to elicit all tetanic contractions. The stimulus amplitude was adjusted, and elicited twitch force determined, in every muscle complex. The lowest stimulus amplitude giving peak twitch force was used for all subsequent contractions. Pulse frequency and train duration were varied for a subset of muscle complexes, and the degree of fusion and force plateau examined. A stimulation

frequency of 80 Hz consistently produced a fused tetanic contraction in which force fluctuations due to individual pulses were < 1% of total force, and a train duration of 350 ms gave a clear force plateau during isometric tetani. Visual inspection of subsequent muscle complexes confirmed that these stimulation parameters produced these effects across all individuals.

## Muscle Isometric Properties

Isometric twitch and tetanic properties of the triceps surae complex were determined. Initially a series of twitches were performed at a range of lengths. The length that yielded peak twitch force was determined, and defined as optimum length ($L_0$). All subsequent contractions were performed at this length, and all forces were corrected for passive force at this length

A subsequent twitch contraction was performed at optimum length. Peak twitch force was determined and time series data were used to calculate the time from onset of activation to peak twitch force ($TP_{tw}$), and the time from peak twitch force to 50% relaxation ($TR_{50}$) (Marsh & Bennett, 1985, 1986; Bennett *et al.*, 1989; Askew & Marsh, 1997; Syme *et al.*, 2005; Nguyen *et al.*, 2020) (Table 1).

Next, an isometric tetanic contraction was performed to determine peak isometric tetanic force ($F_0$) (Table 1). Control isometric tetanic contractions were repeated at regular intervals to monitor muscle complex performance (Holt & Azizi, 2014; Holt *et al.*, 2016). It was pre-established that if force had dropped below 90% of its initial value by the first control isometric tetani (~ $5^{th}$ tetanic contraction), the experiment would be terminated. Large drops in force between the $1^{st}$ and ~$5^{th}$ tetanic contractions resulted in termination of the experiment in 11 mice. We found these HR mice to be particularly sensitive to the effects of both anesthesia and nerve stimulation, hence requiring the exclusion of many mice. However, we believe that the

termination criteria used here allow for minimization of these effects without biasing our sample towards more fatigue-resistant muscle complexes.

Following muscle experiments, muscle complexes were weighed, cross-sectional area calculated (see below), and peak isometric stress calculated as peak isometric tetanic force divided by cross-sectional area. Peak tetanic force ($F_0$) was also normalized to body mass ($F_0$ Mass) to assess the capacity of the muscle complex to support body weight during locomotion (Table 1).

## Muscle Force-Velocity Properties and Curve Fitting

To determine the relationship between muscle complex force and velocity, isotonic tetanic contractions in which the muscle was allowed to shorten, were performed at a range of relative forces (0.1-0.9 $F_0$). Peak shortening velocity was determined at each of these force levels (Supplemental Material 1) and force-velocity curves constructed (Marsh & Bennett, 1985, 1986; Bennett *et al.*, 1989; Askew & Marsh, 1997; Zhan *et al.*, 1999; Syme *et al.*, 2005; Holt *et al.*, 2016; Alcazar *et al.*, 2019; Javidi *et al.*, 2020). For each muscle complex, we performed 13 total contractions, included isotonic shortening contractions and isometric controls, during the force-velocity protocol. This consistency ensured that muscle complexes from all individuals were in the same state at the beginning of the endurance protocol

The force-velocity data were normalized. Active forces in isotonic contractions were divided by peak isometric tetanic force to determine relative force ($F/F_0$). Following muscle experiments, the length of the muscle complex was measured and absolute shortening velocities ($V_{abs}$) were divided by this length to calculate normalized shortening velocity ($V_{norm}$) (Table 1). After plotting the force-velocity points for individual mice, we fitted force-velocity curves using

multiple equations. We initially chose not to rely on a single force-velocity curve fit as none of the commonly used fits have a mechanistic basis, and the force-velocity curves characterized here were relatively linear compared to previously observed curves (see Marsh & Bennett, 1986; Alcazar *et al.*, 2019). We fitted using the Hill rectangular-hyperbola equation: $(P + a)(v + b) = b(P0 + a)$ (Hill, 1938), the Marsh-Bennett hyperbolic linear equation: $V = B(1 – F/F_0) / (A + F/F_0) + C(1 – F/F_0)$ (Marsh & Bennett, 1986; Askew & Marsh, 1997), and a second-order polynomials: $V = Ax^2+Bx+C$. Maximal shortening velocity values were determined (Table 1) for the 3 fits for all mice (Supplemental Material 3), and curves were visually rendered to check for poor fits. Force-velocity data for 4 mice were excluded due to poor curve fits. The force-velocity relationships in these individuals showed negative quadratic fits, whereas the rest of the individuals all had positive quadratic terms.

## Muscle Endurance Properties

The force-generating capacity of the triceps surae muscle complex over repeated isometric tetanic contractions was used to assess muscle endurance (Renaud & Kong, 1991; Zhan *et al.*, 1999; James *et al.*, 2004; Syme *et al.*, 2005). The use of an *in situ* muscle preparation eliminated the effects of the central nervous system while maintaining blood supply and, therefore, provided an assessment of the muscular basis of endurance. The endurance protocol consisted of a standard procedure of repeated isometric tetanic contractions (Allen *et al.*, 2008) elicited using the same stimulation parameters as previous isometric tetanic contractions. One contraction was performed every 5 seconds until force dropped below 50% of its initial value, or for a maximum of 500 contractions. However, due to the high sampling

frequency required, these contractions had to be performed in 10-minute bouts. At the end of each bout the data were saved, and a new bout immediately started.

Peak force in each individual contraction was calculated and plotted against contraction number (~200-500 contractions) (Supplemental Material 2). Endurance ($Endur_{0\text{-}90}$) was quantified as the linear fit (slope) of the decline in force over the first 90 tetanic contractions (Table 1). It was not our intention that this linear descriptor would provide a precise fit to the data. Instead, it provided a comprehensive and comparable way to capture the duration for which initial force can be maintained, the rate of a decline in force, and the point at which force could be sustained, thus allowing comparison across the HR lines. After the first 90 contractions, we quantified the average force that was sustained (Sustained F) over a series of tetanic contractions without a decrease in force (Table 1). We made sure to quantify Sustained F over areas in which force traces were consistently flat and without any peaks (see Results). This sustained force was normalized to peak isometric force measured at the beginning of the experiment (Sustained F/ $F_0$) to quantify the decline in active force given the different levels of initial force across the lines.

## Dissections and Muscle Dimensions

Once the endurance contraction protocol was completed, an overdose of isoflurane anesthesia was administered. The lengths of the Achilles tendon, triceps surae muscle complex (length from the knee joint to the origin of the common Achilles tendon), and muscle-tendon unit were measured to the nearest 0.1 mm with digital calipers while the mouse was still in the stereotaxic frame and the muscle was held at $L_0$. Mice were then removed from the frame,

decapitated, and weighed. The triceps surae complex was dissected free and weighed to the nearest 0.0001 g.

Muscle complex anatomical cross-sectional area (Anatomical CSA) (not accounting for pennation angle or fiber length) was determined from muscle complex mass and length assuming a density of 1060 kg/m$^3$ (Mendez & Keys, 1960) (Table 1). Subsequently, we calculated the peak tetanic stress (stress = $F_0$/CSA) of the triceps surae muscle group (Askew & Marsh, 1997; Zhan *et al.*, 1999; Syme *et al.*, 2005; Holt *et al.*, 2016) (Table 1). Muscle shortening velocities were normalized to muscle length.

# Statistical Analysis

## *Isometric Contractile Properties*

To compare the five groups (4 HR lines, with L6 divided into those with and without the mini-muscle phenotype), we used the MIXED Procedure in SAS (SAS Institute, Cary, NC, USA) to apply analysis of covariance models with age as the covariate. This inclusion of age is necessary due to the large range of ages included in this study (46-107 days old). Analyses of muscle dimensions (except for variables that were normalized) also included body mass as a covariate. We calculated an *a priori* contrast comparing L3 mini and L6 mini with L6, L7, and L8. For post-hoc comparisons within the mini- and within the normal-muscled groups, we examined Differences of Least Squares Means from SAS Procedure MIXED, with adjustment for multiple comparisons. Specifically, we employed Scheffe's procedure because this is the most conservative multiple-range comparison for unequal sample sizes. No data were excluded from isometric contractions, except for $F_0$ Mass for which one low outlier was removed from the analyses. In the endurance protocol we were missing some values of sustained force because

during early experiments, the duration of the endurance protocol required to achieve a reliable value of sustained force was not clear and in a small number of cases, the protocol was stopped prematurely.

### *Force-Velocity Repeated Measures*

Multiple force-velocity points were obtained for each individual mouse, so we used repeated-measures models in SAS Procedure MIXED to test for effects of group on both absolute shortening velocity ($V_{abs}$) and normalized velocity ($V_{norm}$) (Table 2). Covariates were age, relative force ($F/F_0$), and z-transformed relative force squared (orthogonal polynomial used to describe the curvature of the relationship). Individual was treated as a random effect nested within line. Furthermore, we included the interaction between force ($F/F_0$) and group ($F/F_o$*group) to test for differences in slopes. Initially, we also included the interaction between (Zfnorm2) and group (Zfnorm2*group) to test for differences in curvature, but this interaction was not significant, so it was removed from the final model we present.

Least-square means generated from the repeated-measures analyses were estimated at $F/F_0 = 0$ to estimate maximal shortening velocity (mm $s^{-1}$) values from the $2^{nd}$ degree polynomials for both absolute ($V_{max}$) and normalized velocity ($V_{normax}$) (Table 2).

### *Correlations of Muscle Traits*

To examine covariation of muscle complex performance metrics among the five groups, we examined bivariate scatterplots and calculated Pearson pairwise correlation coefficients for $V_{normax}$, $Endur_{0\text{-}90}$, stress, $TP_{tw}$, $TR_{50}$, and Sustained $F/F_0$. We also attempted to calculate correlations while accounting for within-group variation, as indicated by the standard errors, using procedures outlined in Ives et al. (2007), but the data set was too small to achieve reasonable estimates.

## *Results*

Significance levels from ANCOVAs of body mass, muscle complex dimensions, and isometric (tetanic and twitch) properties of the triceps surae complex in HR mice (using body mass and age as a covariate when appropriate) are shown in Figs 1 and 2. Table 2 and Fig. 3 illustrate the results of force-velocity analysis, including representative traces from all groups. Fig. 4 depicts the significance values from the endurance metrics, including representative traces. Table 3 shows the pairwise correlation for the primary muscle contractile characteristics, and Fig. 5 illustrates the significant, negative correlations between velocity and endurance metrics.

## Body Size and Muscle dimensions

Average body mass varied significantly among groups (P=0.0014) (Fig. 1A). With body mass as a covariate, muscle complex length (Fig. 1B), tendon length, and muscle-tendon unit (MTU) length were not significantly different among groups. As expected, relative triceps surae complex mass varied among groups (P<<0.0001) (Fig. 1C), with the mini-muscle mice (L3 Mini and L6 Mini) having significantly lighter muscle complexes (LS Means of 0.052 g and 0.046 g, respectively) when compared with normal-muscled mice (L6=0.105 g, L7=0.095 g, L8=0.114 g) (*a priori* contrast P<<0.0001). *Post hoc* comparisons indicated no statistically significant differences between the two mini-muscle groups or among the three normal-muscle groups. The pattern for anatomical cross-sectional area was similar to that of muscle complex mass (Fig. 1D).

## Isometric Properties

Isometric tetanic stress was not significantly different among groups (Fig. 2A). However, $F_0$ Mass (peak tetanic force normalized to body mass) was significantly different among groups ($P<0.0001$) (Fig. 2B), with the main difference being that mini-muscle mice (L3 Mini and L6 Mini) had significantly lower values (both 0.046 N/g) when compared with the other groups (0.082 N/g for L6, 0.087 N/g for L7, and 0.100 N/g for L8) (*a priori* $P<<0.0001$).

$TP_{tw}$ (s), time from onset of muscle activation to peak twitch force (Table 1), ranged from an average of 0.021 (s) for L3 Mini to 0.025 (s) for L6 Mini but was not significantly different among groups (Fig. 2C). $TR_{50}$, time from peak twitch force to half relaxation (Table 1) also did not differ among groups (Fig. 2D).

## Force-Velocity Properties

Fig. 3 depicts force-velocity traces from a representative mouse from each group, along with the second order polynomial curve-fits (see Methods). This curve fit was deemed to provide the most reliable fit for the force-velocity points and estimation of maximal shortening velocity ($V_{max}$) (Fig. 3A-3E). The Hill equation forced a curve when none existed, and the Marsh-Bennett equation often generated convex shapes (Supplemental Material 3).

For absolute velocity ($V_{abs}$), the effect of group was highly significant (both $P<<0.0001$), as was the effect of relative force ($F/F_0$) (both $P<<0.0001$), the z-transformation of force ($F/F_0$) (ZFnorm2) ($P<<0.0001$), and the interaction between $F/F_o$ and group ($P<<0.0001$) (Table 2). The interaction between $F/F_o$ and group indicates differences in slope of the F-V curve among the groups. The *a priori* contrast between $V_{max}$ for mini- and normal-muscled groups was highly significant ($P<< 0.0001$). In addition, the post hoc comparisons indicated that $V_{max}$ in L8 was

447 significantly higher than L6 (P=0.0005) and L7 (P<<0.0001). Results were similar for
448 normalized velocity ($V_{norm}$) (Table 2).
449

## 450 Endurance Properties

451 Fig. 4 illustrates the endurance protocol for representative mice from each of the five
452 groups. The slight recovery in active force every 100 contractions is due to the need to save data
453 and restart the protocol, thus giving the muscle a slightly longer recovery time. In L3 Mini and
454 L6 Mini individuals there was a minimal drop in active force over the entire endurance protocol
455 as compared with the other three groups (e.g., Fig. 4A and 4B versus Fig. 4C, 4D, 4E). $Endur_{0\text{-}90}$
456 (the slope of the decline in force over the first 90 tetanic contractions) was significantly different
457 among groups (P<<0.0001), being shallowest in the mini-muscle mice (L3 Mini=-0.00348, L6
458 Mini=-0.00238), steepest in normal lines L6 and L8 (-0.01676 and -0.01853, respectively), and
459 intermediate in L7 (-0.01145) (Fig. 4F). The *a priori* contrast between mini- and normal-
460 muscled groups was highly significant (P<<0.0001). Sustained $F/F_0$ also differed among groups
461 (P<0.0001), with mini-muscle groups having higher values (0.98 for L3 Mini and 0.92 for L6
462 Mini) when compared with L6 (0.44), L7 (0.47), and L8 (0.36) groups (Fig. 4G). The *a priori*
463 contrast between mini- and normal-muscled groups was also highly significant (P<<0.0001).
464

## 465 Pairwise Pearson's Correlations

466 Table 3 provides correlations for the five groups Least Squares Means for normalized
467 maximum shortening velocity ($V_{normax}$), endurance ($Endur_{0\text{-}90}$, Sustained $F/F_0$), and isometric
468 properties (stress, $TP_{tw}$, $TR_{50}$). Of the 15 correlations, the correlations between $V_{normax}$ and
469 $Endur_{0\text{-}90}$ (r = -0.993), $V_{normax}$ and Sustained $F/F_0$ (-0.971), and Sustained $F/F_0$ and $Endur_{0\text{-}90}$

(0.961) were statistically significant (P<0.01) (Table 3, Fig. 5). Mini-muscle mice (L3 Mini and L6 Mini) have the highest endurance ($Endur_{0\text{-}90}$ and Sust. $F/F_0$) but slowest muscle complexes ($V_{normax}$), L6 and L8 have the lowest endurance but fastest muscle complexes, and L7 is intermediate.

## *Discussion*

The purpose of the present study was to test whether a muscle-level trade-off underlies the negative relationship between the duration of daily wheel running and the average running speed, that was previously observed to have evolved among four replicate lines of High Runner (HR) mice (Garland *et al.*, 2011). We used an *in situ* preparation of the triceps surae complex to determine muscle isometric, force-velocity, and endurance properties. Although we found a negative relationship between muscle complex speed and endurance (Fig. 5A+B), indicative of a muscle-level trade-off, the ordering among lines (groups) was reversed as compared with wheel-running behavior (Garland *et al.*, 2011).

## Muscle Dimensions

The only reported difference in muscle dimensions across our HR groups was the previously reported ~50% reduction in triceps surae muscle complex mass in mini-muscle mice when compared with normal-muscled individuals (Fig. 1C) (Garland *et al.*, 2002; Houle-Leroy *et al.*, 2003; Syme *et al.*, 2005). Given that there was no statistical difference in muscle length across all groups, anatomical cross-section area was therefore also significantly reduced in the mini-muscle groups (Fig. 1).

## Isometric Properties

Isometric tetanic stress ranged from an average of 25.9 N/cm$^2$ for L6 to 36.6 N/cm$^2$ for L8, but was not significantly different among groups. This calculation of stress (Table 1, Fig. 2A) was based on the anatomical CSA of the triceps surae complex. The lower value of anatomical, as opposed to physiological, cross-sectional area, will lead to higher estimates of stress. Previous studies of isolated muscles from HR mice have reported values of 16.7-17.8 N/cm$^2$ for the medial gastrocnemius muscle (Zhan *et al.*, 1999), and 16.7-29.5 N/cm$^2$ and 33.3-38.1 N/cm$^2$ for isolated medial gastrocnemius and soleus muscles respectively (Syme *et al.*, 2005). Studies of isolated calf muscles (soleus and extensor digitorium longus) in CD-1 mice reported variable stress values that depended on age and fatigue (James *et al.*, 2004; Hill *et al.*, 2020), but were on average lower than stress values for the triceps surae complex reported here. Although our study of the entire triceps surae complex best allows us to examine muscle properties as they pertain to locomotion, it also means that we cannot attribute force contributions to individual muscles, calculate physiological cross-sectional areas of each of these morphological distinct muscles, nor determine stress in each individual muscle.

In addition to normalizing isometric tetanic force of the triceps surae complex to its anatomical cross-sectional area, we also normalized it to body mass to enable us to assess the capacity of this muscle group to support body weight during locomotion. Muscle force relative to body mass was significantly lower in mini-muscle mice than normal-muscle mice (Fig. 1B), which may contribute to the reduced maximal sprint speed previously observed in these groups (Dlugosz *et al.*, 2009).

514 Rates of force development and relaxation were determined from isometric twitches.
515 Time from muscle complex activation to peak twitch force ranged from an average of 0.021 (s)
516 for L3 Mini to 0.025 (s) for L6 Mini, but was not significantly different among groups (Fig. 2C).
517 $TR_{50}$ ranged from 0.012 s for L7 to 0.013 s for L8, and was also not significantly different among
518 groups. Force rise times are a little slower than the 0.016 s measured in isolated soleus muscles
519 from ICR outbred mice, while the half relaxation times are slightly faster (0.023 s reported
520 previously) (Askew and Marsh, 1997). The lack of difference between our 5 groups is somewhat
521 in contrast with a previous study comparing only mini-muscle and normal-muscle groups of
522 mice. Syme *et al*. (2005) showed a shorter entire twitch duration (measured at 50% of peak
523 force) and relaxation time (measured from 90% to 10% of peak force) in the soleus from L6
524 Mini compared to the soleus from either L3 Mini or L6 Normal, and a shorter relaxation time
525 (measured from 90% to 10% of peak force) in the medial gastrocnemius muscle from L6 Normal
526 mice compared to either of the mini-muscle groups.
527 Faster relaxation times are not surprising given that we examined not only the slow
528 soleus, but also the plantaris and medial and lateral gastrocnemius muscles, which are known to
529 have a larger proportion of faster fibers (Zhan *et al.*, 1999; Houle-Leroy *et al.*, 2003; Guderley *et*
530 *al.*, 2006; McGillivray *et al.*, 2009; Schaeffer & Lindstedt, 2013; Talmadge *et al.*, 2014). The
531 slower rate of force development, and the lack of difference across our 5 groups, are harder to
532 explain. However, they may be a consequence of using the entire triceps surae complex
533 containing multiple muscles, and significant series compliance in the Achilles tendon and
534 aponeuroses. The use of multiple muscles within this complex may mean that any effects, such
535 as loss of type IIb fibers in the gastrocnemius muscles of mini-muscle mice (Guderley *et al.*,
536 2006; Talmadge *et al.*, 2014) and the slower relaxation this presumably caused (Syme et al.,

2005), are obscured or counteracted by the effects of the mini-muscle phenotype on other muscles, such as the faster twitch kinetics in the soleus (Syme et al., 2005). In addition, the presence of series compliance will have slowed the time course of force generation (Hill, 1951; Mayfield *et al.*, 2016), and may potentially have obscured any differences in rate of fiber force generation across the groups. Hence, the use of the entire triceps surae complex limits our ability to identify changes in individual muscles. However, it demonstrates that any variation in the properties of individual muscles across HR lines will likely not have affected the rate of force generation at the ankle during locomotion, and that this rate may be lower than that predicted by isolated muscle kinetics.

## Force-Velocity Properties

Estimated maximum shortening velocity ($V_{max}$) and slope, but not curvature, of the force-velocity relationship varied across our 5 groups of HR mice. $V_{max}$ was lowest in mini-muscle mice (L3 Mini=25.2, L6 Mini=25.5 mm $s^{-1}$), highest in L8 (50.3 mm $s^{-1}$), and intermediate in L6 and L7 (40.4 and 37.2 mm $s^{-1}$ respectively) (Fig. 3). The values of $V_{max}$ reported here are somewhat lower than have previous been documented in both isolated muscles from a subset of HR groups, ~62-65 mm $s^{-1}$ and ~60-70 mm $s^{-1}$ in isolated soleus and medial gastrocnemius muscles respectively (Syme *et al*., 2005), and in other non-HR soleus muscles where values ~60-65 mm $s^{-1}$ have been reported (Asmussen & Maréchal, 1989; Maréchal & Beckers-Bleukx, 1993; Askew & Marsh, 1997). In addition, we report significant differences in $V_{max}$, without any difference in the curvature of the force-velocity relationship. This is in contrast to a previous study on a subset of HR groups that showed a difference in curvature, in the absence of a

559 difference in $V_{max}$, between medial gastrocnemius muscles from mini-muscle and normal-muscle
560 mice (Syme *et al*., 2005).

561 The overall lower values of $V_{max}$ reported here may have several explanations. It may be
562 partially a consequence of our force-velocity curve fitting; the relatively flat force-velocity
563 relationships measured here were fit better by a second-order polynomial, than by traditional
564 curve fitting equations. This approach may have reduced the estimate of $V_{max}$ compared to other
565 curve-fitting methods (Supplementary Materials 3). However, it is possible that the relatively
566 low value of $V_{max}$ also reflects a shift in contractile properties in all HR lines compared to non-
567 HR mice, and potentially a greater shift than earlier generations of HR mice (Syme et al., 2005),
568 due to prolonged selection for high levels of voluntary wheel running.

569 It is unclear why the data presented here show different values of $V_{max}$ between muscle
570 complexes from mini-muscle and normal-muscle lines, in addition to differences between
571 normal-muscle HR lines, when Syme et al., (2005) did not find any such differences. It seems
572 unlikely that using the whole triceps surae complex as opposed to individual muscles would lead
573 to this finding - different effects of the mini-muscle phenotype on the various muscles in the
574 complex would be more likely to cancel out than lead to difference between groups. Possibly
575 these effects are also a consequence of differences in curve fitting procedure, or potentially
576 continued responses to ongoing selective breeding over tens of generations.

577 Syme *et al*. (2005) also demonstrated a greater curvature in the medial gastrocnemius
578 muscles of mini-muscle groups compared to normal-muscle groups. The curvature of the force-
579 velocity relationship varies from linear to double-hyperbolic, with the reasons for these
580 differences being poorly understood (Alcazar et al., 2019). Hence, it is conceivable than the

linearity of the curves measured in this study is a consequence of measuring only the summed output of multiple muscles with different fiber type compositions and morphologies.

Any difference in $V_{max}$ and curvature of the force-velocity relationship that are not simply a consequence of curve-fitting procedures, or the measurement of the properties of the entire muscle complex, are likely a reflection of changes in muscle fiber type composition (Schiaffino & Reggiani, 2011). The only study to date that has investigated differences in myosin isoform composition amongst HR lines was at generation 46, and compared soleus, plantaris, and gastrocnemius muscles in L3 Mini, L7 and L8 mice. That study reported the soleus had a slightly higher proportion of faster myosin isoforms in the L3 mini-muscle mice, whereas the gastrocnemius and plantaris muscles had a marked reduction in faster myosin isoforms (McGillivray *et al.*, 2009). The large losses of faster fiber types in the mini-muscle lines are consistent with the lower $V_{max}$ values reported in these groups here. However, the lack of difference in myosin isoforms between L7 and L8 at generation 46 (McGillivray *et al.*, 2009) are not consistent with the difference in $V_{max}$ between these lines reported here (Fig. 3). This may reflect subtle changes not detectable by myosin isoform analysis, or ongoing changes in these groups since generation 46.

## Endurance Properties

The soleus and medial gastrocnemius muscles in mice generally fatigue within the first 100 tetanic contractions (Brooks *et al.*, 2018; Cabelka *et al.*, 2019) or within 100-500 seconds (e.g., see Pagala *et al.*, 1998; Zhao *et al.*, 2005), with the soleus generally being more fatigue-resistant. Such differences in muscle fatigue are, at least in part, attributed to muscle fiber type composition, with Type I fiber abundance being positively correlated with fatigue resistance (see

604 references in Garland, 1988; Schiaffino & Reggiani, 2011). The first study examining endurance
605 properties in muscles from HR mice was at generation 10, and while voluntary exercise on
606 wheels for 2 months improved muscle fatigue-resistance, no significant differences were found
607 between HR and C mice (mini-muscle individuals were not present in the sample) (Zhan *et al.*,
608 1999). Subsequently, Syme *et al*. (2005) reported that the medial gastrocnemius muscle in mini-
609 muscle individuals had significantly slower rates of fatigue for both isometric force and cyclic
610 net work.

611 In the present study we determined endurance *in situ*, in the presence of a functioning
612 circulatory system, across 5 groups of HR mice. Endurance, measured as the slope of the decline
613 in force over the first 90 tetanic contractions ($Endur_{0\text{-}90}$), varied significantly in the triceps surae
614 muscle complex, being shallowest in the mini-muscle mice (L3 Mini=-0.00348, L6 Mini=-
615 0.00238), steepest in lines L6 and L8 (-0.01676 and -0.01853), and intermediate in L7 (-0.01145)
616 (Fig. 4F). Sustained $F/F_0$ (sustained isometric force normalized to peak tetanic force) was
617 higher in mini-muscle mice (Fig. 4G), likely due to the higher prevalence of fatigue-resistant
618 muscle fibers (McGillivray *et al.*, 2009; Talmadge *et al.*, 2014). Although the mini-muscle
619 phenotype has drastic effects on muscular endurance, L7 mice also have evolved to have greater
620 endurance as compared to the other normal-muscled HR lines (Fig. 4). As with changes to the
621 force-velocity properties of this line, this was not reflected in fiber type composition at
622 generation 46, and likely represents either subtle changes that could not be detected using the
623 study of myosin isoforms or subsequent changes since generation 46.

624

625 # Trade-offs and Experimental Studies

626 Despite the clear rationale for, and evolutionary importance of, organismal-level speed-
627 endurance trade-offs underpinned by muscle-level trade-offs, experimental evidence is
628 inconsistent. On one hand, trade-offs at the muscle level can sometimes be related to
629 organismal-level performance trade-offs. For example, organismal level trade-offs in the "roll-
630 snap" behavior (the rapid snapping of their wings together above their back) of bearded
631 manakins can be partly explained by contraction-relaxation cycling kinetics in the skeletal
632 muscle that actuates the display (Miles *et al.*, 2018). On the other hand, trade-offs at the level of
633 subordinate traits, such as muscles, can be at odds with speed and endurance metrics at the
634 organismal level. For example, at the organismal-level, one study reported an absence of a trade-
635 off between burst swimming performance and endurance capacity in African clawed frogs
636 (Wilson *et al.*, 2002), and another found only marginal evidence for a trade-off between burst
637 (speed and acceleration) and sustained locomotion in lacertid lizards (Vanhooydonck *et al.*,
638 2014). At the muscle-level, studies of these same specimens have revealed highly significant
639 trade-offs between muscular power output and fatigue resistance (Wilson *et al.*, 2002;
640 Vanhooydonck *et al.*, 2014). Selection experiments, in which conditions are tightly controlled,
641 may help to resolve the extent to which these trade-offs could exist and be evolutionarily
642 important.
643

644 # Experimental Evolution and Trade-offs in HR mice

645 Selection experiments and experimental evolution can be used to study evolution in real time by
646 determining the sequence of phenotypic and behavioral changes that occur during adaptation to a
647 defined selective regime (Garland, 2003; Garland & Rose, 2009; Marchini *et al.*, 2014;
648 Biesiadecki *et al.*, 2020). For example, functional trade-offs involving both muscle and bone

649 underlie trade-offs between running and fighting ability that emerged as greyhounds and pit bulls
650 were developed by artificial selection (Pasi & Carrier, 2003; Kemp *et al.*, 2005). However, few
651 studies have used these approaches to elucidate mechanisms that underlie trade-offs, or examine
652 discrepancies between trade-offs at the organismal level and those found among lower-level
653 traits.

654 A significant negative correlation between average running speed and time spent running
655 on wheels among the four replicate HR lines was reported at generation 43 (Garland *et al.*,
656 2011). L3 mini-muscle mice (mini-muscle status was unknown for L6) ran for the fewest
657 minutes per day on wheels, but at the highest average speeds. Mice from L8 ran for the longest
658 durations, but at the slowest average speeds. Line 7 was intermediate for both speed and
659 duration of wheel running.

660 The muscle complex data presented here for the HR lines from this selection experiment
661 demonstrate a trade-off between muscle speed and endurance across groups (Table 3; Fig. 5).
662 However, this muscle-level trade-off is the opposite of that seen at the organismal-level (Garland
663 *et al.*, 2011). Mini-muscle mice (L3 Mini and L6 Mini) had the highest endurance ($Endur_{0\text{-}90,}$
664 Sustained $F/F_0$) but slowest muscle complexes ($V_{norm}$), L6 and L8 had the lowest endurance but
665 fastest muscles, and L7 was intermediate. Hence, although both muscle (Fig. 5) and organismal
666 (Garland *et al.*, 2011) level trade-offs between speed and endurance have been observed across
667 HR lines, the former may not underpin the latter.

668 Muscle and organismal level trade-offs might not reflect one another for various reasons.
669 Firstly, it is important to note that the apparent reversal of the ordering in muscle and organismal
670 level trade-offs (Fig.5; Garland *et al.*, 2011) may not actually be as much of a discrepancy as it
671 initially appears. Maximal running speeds on wheels (Roach *et al.*, 2012) are well below

maximal sprint speeds (Dohm *et al.*, 1996; Girard *et al.*, 2001; Dlugosz *et al.*, 2009; Claghorn *et al.*, 2017), and maximal sprint speed is reduced in L3 Mini individuals as compared with L7 and L8 individuals (Dlugosz *et al.*, 2009). Hence, if we had measured sprint speed (Dlugosz *et al.*, 2009) and running endurance (Meek *et al.*, 2009) as metrics of organismal-level speed and endurance in this generation, we may not have found any evidence of a trade-off. This would be more in line with previous studies that show evidence of muscle-level trade-off, but no, or marginal, trade-offs at the organismal-level (Wilson *et al.*, 2002; Vanhooydonck *et al.*, 2014). However, the potential to draw different conclusions regarding trade-offs at submaximal and maximal activity levels highlights the complexity of trade-off studies (for a general review of this, see Garland *et al.*, 2022), and calls into question the relationship between muscle properties and organismal performance during submaximal tasks.

Hence, there is potential for there not to be a complete reversal of muscle and organismal level trade-offs if different organismal-level metrics were used. However, it does still seem likely that there is some degree of discrepancy. An obvious potential cause of differences between muscle and organismal level traits is that muscle properties are only one of many lower-level traits that contribute to whole-animal locomotor abilities. Although metrics of maximal sprint speed are relatively closely related to aspects of muscle properties among human athletes (e.g., see Komi, 1984), other morphological, neural, and biomechanical traits are also important. And measures of endurance encompass many additional lower-level traits besides muscle physiology, including biomechanics, oxygen transport and delivery, thermoregulatory abilities, and additional cellular biochemical processes (discussed in Garland, 1988; Jones & Lindstedt, 1993; Schiaffino & Reggiani, 2011; Vanhooydonck *et al.*, 2014; Thompson, 2017). Higher-level factors, such as differences in motivation, are also likely to have major effects on running speed

and duration (e.g., see Rhodes *et al.*, 2005; Claghorn *et al.*, 2016; Garland *et al.*, 2016; Roberts *et al.*, 2017; Saul *et al.*, 2017 and references therein).

Although many of the factors mentioned above are beyond the scope of this study, here we consider in more detail the potential for muscle and biomechanical factors to obscure the effects of muscle-level trade-offs, as a significant amount of literature exists on these topics in the HR mice. Individuals may, at least in part, compensate for the functional constraints that particular muscles impose by activating additional agonistic muscles (discussed in Wilson & James, 2004), and changing their gait. HR mice have evolved narrower stance width than C mice lines, mini-muscle mice have increased duty factor and larger paw contact areas (Claghorn *et al.*, 2017), and female HR mice run more intermittently than C mice (Girard *et al.*, 2001).

One specific example of how the intersection of muscle and biomechanical factors could potentially contribute to discrepancies between muscle (Fig. 5) and organismal level (Garland *et al.*, 2011) trade-offs is the reduced capacity of the triceps surae to support body weight in mini-muscle lines (Fig. 2B). Locomotor endurance is determined not only by the fatigue resistance of the muscle fibers, but also the total force capacity of the muscle relative locomotor demands. The reduced capacity of the triceps surae of mini-muscle mice to support body weight likely reduces the reserve capacity of the muscular system, meaning that any fatigue of the individual fibers will likely have a greater contribution to organismal fatigue. However, this effect may be offset by further biomechanical changes in mini-muscle mice, such as higher duty factors (Claghorn *et al.*, 2017), which reduce peak force demands during running. Hence, while reduced muscle reserve certainly isn't a definitive explanation for the discrepancies seen between muscle and organismal levels, but it does highlight the emergent nature of organismal performance, and

717 the limited role that any given tissue-level trade-offs may play, particularly during submaximal
718 activities.

719

720 ## *Acknowledgements*

721 We thank members of the Garland lab for helping to obtain the animals used here, Allyn
722 Nguyen for helpful discussions, and Anthony R. Ives and David A. Hillis for help with statistical
723 analyses. Supported by U.S. National Science Foundation grant IOS-1121273 to T.G. and N.H.

724

725

726

## *Competing Interests*

The authors declare no competing or financial interests.

## *Author Contributions*

A.A.C., T.G., and N.C.H designed the experiments. A.A.C, S.A., and N.C.H. conducted the experiments and collected data. A.A.C. T.G., and S.A. analyzed the data. A.A.C. drafted the manuscript. A.A.C., T.G., and N.C.H revised and edited the manuscript. All authors approved the final version of the manuscript.

## *Funding*

Supported by National Science Foundation grant IOS-2038528 to T.G. and N.C.H.

## *Data Availability*

Data are available on request from the authors.

# *References*


**Ackerly, D.D., Dudley, S.A., Sultan, S.E., Schmitt, J., Coleman, J.S., Linder, C.R., Sandquist, D.R., Geber, M.A., Evans, A.S., Dawson, T.E. and Lechowicz, M.J.** (2000). The evolution of plant ecophysiological traits: Recent advances and future directions. *BioScience* **50**, 979.

**Agrawal, A.A.** (2020). A scale-dependent framework for trade-offs, syndromes, and specialization in organismal biology. *Ecology* **101**, e02924.

**Albuquerque, R.L., Bonine, K.E. and Garland Jr., T.** (2015). Speed and endurance do not trade off in Phrynosomatid lizards. *Physiol. Biochem. Zool.* **88**, 634–647.

**Alcazar, J., Csapo, R., Ara, I. and Alegre, L.M.** (2019). On the shape of the force-velocity relationship in skeletal muscles: The linear, the hyperbolic, and the double-hyperbolic. *Front. Physiol.* **10,** 769

**Allen, D.G., Lamb, G.D. and Westerblad, H.** (2008). Skeletal muscle fatigue: Cellular mechanisms. *Physiol. Rev.* **88,** 287–332.

**Askew, G.N. and Marsh, R.L.** (1997). The effects of length trajectory on the mechanical power output of mouse skeletal muscles. *J. Exp. Biol.* **200,** 3119–3131.

**Asmussen, G. and Maréchal, G.** (1989). Maximal shortening velocities, isomyosins and fibre types in soleus muscle of mice, rats and guinea-pigs. *J. Physiol.* **416,** 245–254.

**Barclay, C.J.** (2005) Modelling diffusive $O_2$ supply to isolated preparations of mammalian skeletal and cardiac muscle. *J. Mus. Res. Cell Mot.* **26,** 225-235

**Bennett, A.F., Garland Jr., T. and Else, P.L.** (1989). Individual correlation of morphology, muscle mechanics, and locomotion in a salamander. *Am. J. Physiol.-Regul. Integr. Comp. Physiol.* **256**, R1200–R1208.

**Biesiadecki, B.J., Brotto, M.A., Brotto, L.S., Koch, L.G., Britton, S.L., Nosek, T.M. and Lin, J-P.** (2020). Rats genetically selected for low and high aerobic capacity exhibit altered soleus muscle myofilament functions. *Am. J. Physiol.Cell Physiol.* **318,** C422–C429.

**Bonine, K.E., Gleeson, T.T. and Garland Jr., T.** (2005). Muscle fiber-type variation in lizards (Squamata) and phylogenetic reconstruction of hypothesized ancestral states. *J. Exp. Biol.* **208,** 4529–4547.

**Brooks, M.J., Hajira, A., Mohamed, J.S. and Alway, S.E.** (2018). Voluntary wheel running increases satellite cell abundance and improves recovery from disuse in gastrocnemius muscles from mice. *J. Appl. Physiol.* **124,** 1616–1628.

**Cabelka, C.A., Baumann, C.W., Collins, B.C., Nash, N., Le, G., Lindsay, A., Spangenburg, E.E. and Lowe, D.A.** (2019). Effects of ovarian hormones and estrogen receptor α on physical activity and skeletal muscle fatigue in female mice. *Exp. Gerontol.* **115**, 155–164.

**Cadney, M.D., Hiramatsu, L., Thompson, Z., Zhao, M., Kay, J.C., Singleton, J.M., Alburqueque, R.L., Schmill, M.P., Saltzman, W. and Garland Jr., T.** (2021). Effects of early-life exposure to Western diet and voluntary exercise on adult activity levels, exercise physiology, and associated traits in selectively bred High Runner mice. *Physiol. Behav.* **234**, 113389.

**Careau, V. and Wilson, R.S.** (2017). Performance trade-offs and ageing in the 'world's greatest athletes.' *Proc. R. Soc. B Biol. Sci.* **284**, 20171048.

**Careau, V., Wolak, M.E., Carter, P.A. and Garland Jr., T.** (2013). Limits to behavioral evolution: The quantitative genetics of a complex trait under directional selection. *Evolution* **67**, 3102–3119.

**Castro, A. A., F. A. Karakostis, L. E. Copes, H. E. McClednon, A. P. Trivedi, N. E. Schwartz, and T. Garland, Jr.** (2022). Effects of selective breeding for voluntary exercise, chronic exercise, and their interaction on muscle attachment site morphology in house mice. *J. Anat.* **240**, 279–295.

**Claflin, D.R. and Faulkner, J.A.** (1989). The force-velocity relationship at high shortening velocities in the soleus muscle of the rat. *J. Physiol.* **411,** 627–637.

**Claghorn, G.C., Fonseca, I.A.T., Thompson, Z., Barber, C. and Garland Jr., T.** (2016). Serotonin-mediated central fatigue underlies increased endurance capacity in mice from lines selectively bred for high voluntary wheel running. *Physiol. Behav.* **161,** 145–154.

**Claghorn, G.C., Thompson, Z., Kay, J.C., Ordonez, G., Hampton, T.G. and Garland Jr., T.** (2017). Selective breeding and short-term access to a running wheel alter stride characteristics in house mice. *Physiol. Biochem. Zool.* **90,** 533–545.

**Cohen, A.A., Coste, C.F.D., Li, X., Bourg, S. and Pavard, S.** (2020). Are trade-offs really the key drivers of ageing and life span? *Funct. Ecol.* **34,** 153–166.

**Dlugosz, E.M., Chappell, M.A., McGillivray, D.G., Syme, D.A. and Garland Jr., T.** (2009). Locomotor trade-offs in mice selectively bred for high voluntary wheel running. *J. Exp. Biol.* **212**, 2612–2618.

**Dohm, M.R., Hayes, J.P. and Garland Jr., T.** (1996). Quantitative genetics of sprint running speed and swimming endurance in laboratory house mice *Mus domesticus*. *Evolution* **42,** 355–350.

**Esbjörnsson, M., Sylvén, C., Holm, I. and Jansson, E.** (1993). Fast twitch fibres may predict anaerobic performance in both females and males. *Int. J. Sports Med.* **14,** 257–263.

**Garland Jr., T.** (1988). Genetic basis of activity metabolism. I. Inheritance of speed, stamina, and antipredator displays in the Garter Snake *Thampnophis Sirtalis*. *Evolution* **42**, 335-350

**Garland Jr., T.** (2003). Selection experiments: An under-utilized tool in biomechanics and organismal biology. In: *Vertebrate Biomechanics and Evolution*. Oxford, UK: Bios Scientific Publisher,.

**Garland Jr., T. and Carter, P.A.** (1994). Evolutionary Physiology. *Annu. Rev. Physiol.* **56,** 579–621.

**Garland Jr., T., Downs, C. and Ives, A.R.** (2022). Invited Perspective: Trade-offs (and constraints) in organismal biology. *Physiol. Biochem. Zool.* **95,** 82–112.

**Garland Jr., T., Kelly, S.A., Malisch, J.L., Kolb, E.M., Hannon, R.M., Keeney, B.K., Van Cleave, S.L. and Middleton, K.M.** (2011). How to run far: Multiple solutions and sex-specific responses to selective breeding for high voluntary activity levels. *Proc. R. Soc. B Biol. Sci.* **278,** 574–581.

**Garland Jr., T., Morgan, M.T., Swallow, J.G., Rhodes, J.S., Girard, I., Belter, J.G. and Carter, P.A.** (2002). Evolution of a small-muscle polymorphism in lines of house mice selected for high activity levels. *Evolution* **56,** 1267–1275.

**Garland Jr., T. and Rose, M.R.** (eds). (2009). *Experimental evolution: Concepts, methods, and applications of selection experiments*. Berkeley, CA: University of California Press,.

**Garland Jr., T., Zhao, M. and Saltzman, W.** (2016). Hormones and the evolution of complex traits: Insights from artificial selection on behavior. *Integr. Comp. Biol.* **56,** 207–224.

**Girard, I., McAleer, M.W., Rhodes, J.S. and Garland Jr., T.** (2001). Selection for high voluntary wheel-running increases speed and intermittency in house mice *(Mus domesticus)*. *J. Exp. Biol.* **204,** 4311–4320.

**Gleeson, T.T. and Harrison, J.M.** (1988). Muscle composition and its relation to sprint running in the lizard *Dipsosaurus dorsalis*. *Am. J. Physiol. Regul. Integr. Comp. Physiol.* **255,** R470–R477.

**Goodman, B.A., Krockenberger, A.K. and Schwarzkopf, L.** (2007). Master of them all: Performance specialization does not result in trade-offs in tropical lizards. *Evol. Ecol. Res.* **9,** 527–546.

**Guderley, H., Houle-Leroy, P., Diffee, G.M., Camp, D.M. and Garland Jr., T.** (2006). Morphometry, ultrastructure, myosin isoforms, and metabolic capacities of the “mini muscles” favoured by selection for high activity in house mice. *Comp. Biochem. Physiol. B Biochem. Mol. Biol.* **144,** 271–282.

**Henneman, E.** (1957) Relation between size of neurons and their susceptibility to discharge. *Science* **126,** 1345–1347.

**Herrel, A. and Bonneaud, C.** (2012). Trade-offs between burst performance and maximal exertion capacity in a wild amphibian, *Xenopus tropicalis*. *J. Exp. Biol.* **215,** 3106-3111

**Herrel, A., Podos, J., Vanhooydonck, B. and Hendry, A.P.** (2009). Force-velocity trade-off in Darwin's finch jaw function: A biomechanical basis for ecological speciation? *Funct. Ecol.* **23,** 119–125.

**Hill, A.V.** (1951). The effect of series compliance on the tension developed in a muscle twitch. *Proc. R. Soc. Lond. B Biol. Sci.* **138,** 325–329.

**Hill, A.V.** (1938). The heat of shortening and the dynamic constants of muscle. *Proc. R. Soc. Lond. B Biol. Sci.* **126,** 136–195.

**Hill, C., James, R.S., Cox, V.M., Seebacher, F. and Tallis, J.** (2020). Age-related changes in isolated mouse skeletal muscle function are dependent on sex, muscle, and contractility mode. *Am. J. Physiol. Regul. Integr. Comp. Physiol.* **319**, R296–R314.

**Hillis, D., Yadgary, L., Weinstock, G. M., Pardo−Manuel de Villena, F., Pomp, D., Fowler, A., Xu, S., Chan, F., and Garland, Jr, T.** (2020). Genetic basis of aerobically supported voluntary exercise: results from a selection experiment with house mice. *Genetics* **216,** 781–804.

**Hiramatsu, L.** (2017). Physiological and genetic causes of a selection limit for voluntary wheel-running in mice. *PhD thesis*, University of California, Riverside, Riverside, CA.

**Hiramatsu, L., Kay, J.C., Thompson, Z., Singleton, J.M., Claghorn, G.C., Albuquerque, R.L., Ho, B., Ho, B., Sanchez, G. and Garland Jr., T.** (2017). Maternal exposure to Western diet affects adult body composition and voluntary wheel running in a genotype-specific manner in mice. *Physiol. Behav.* **179,** 235–245.

**Hodson-Tole, E.F. and Wakeling, J.M.** (2008) Motor unit recruitment patterns 1: responses to changes in locomotor velocity and incline. *J. Exp. Biol.* **211**, 1882-1892

**Holt, N.C. and Azizi, E.** (2014). What drives activation-dependent shifts in the force–length curve? *Biol. Lett.* **10**, 20140651.

**Holt, N.C., Danos, N., Roberts, T.J. and Azizi, E.** (2016). Stuck in gear: Age-related loss of variable gearing in skeletal muscle. *J. Exp. Biol.* **219,** 998–1003.

**Houle-Leroy, P., Guderley, H., Swallow, J.G. and Garland Jr., T.** (2003). Artificial selection for high activity favors mighty mini-muscles in house mice. *Am. J. Physiol. Regul. Integr. Comp. Physiol.* **284,** R433–R443.

**Ives, A.R., Midford, P.E. and Garland Jr., T.** (2007). Within-species variation and measurement error in phylogenetic comparative methods. *Syst. Biol.* **56,** 252–270.

**James, R.S., Wilson, R.S. and Askew, G.N.** (2004). Effects of caffeine on mouse skeletal muscle power output during recovery from fatigue. *J. Appl. Physiol.* **96,** 545–552.

**Javidi, M., McGowan, C.P. and Lin, D.C.** (2020). Estimation of the force-velocity properties of individual muscles from measurement of the combined plantar flexor properties. *J. Exp. Biol.* **223**, jeb.219980.

**Jones, J.H. and Lindstedt, S.L.** (1993). Limits to maximal performance. *Annu. Rev. Physiol.* **55,** 547–569.

**Kemp, T.J., Bachus, K.N., Nairn, J.A. and Carrier, D.R**. (2005). Functional trade-offs in the limb bones of dogs selected for running versus fighting. *J. Exp. Biol.* **208,** 3475–3482.

**Kolb, E.M., Kelly, S.A. and Garland Jr., T.** (2013). Mice from lines selectively bred for high voluntary wheel running exhibit lower blood pressure during withdrawal from wheel access. *Physiol. Behav.* **112–113,** 49–55.

**Kolb, E.M., Kelly, S.A., Middleton, K.M., Sermsakdi, L.S., Chappell, M.A. & Garland Jr., T.** (2010). Erythropoietin elevates $VO_{2max}$ but not voluntary wheel running in mice. *J. Exp. Biol.* **213,** 510–519.

**Komi, P.V.** (1984). Physiological and biomechanical correlates of muscle function: effects of muscle structure and stretch-shortening cycle on force and speed. *Exerc. Sport Sci. Rev.* **12,** 81–121.

**Liddell, E.G.T., Sherrington, C.S.** (1925) Recruitment and some other factors of reflex inhibition. *Proc. R. Soc. Lond. B* **97,** 488–518

**Marchini, M., Sparrow, L.M., Cosman, M.N., Dowhanik, A., Krueger, C.B., Hallgrimsson, B. and Rolian, C.** (2014). Impacts of genetic correlation on the independent evolution of body mass and skeletal size in mammals. *BMC Evol. Biol.* **14,** 258.

**Maréchal, G. and Beckers-Bleukx, G.** (1993). Force-velocity relation and isomyosins in soleus muscles from two strains of mice (C57 and NMRI). *Eur. J. Physiol.* **424,** 478–487.

**Marsh, R.L. and Bennett, A.F.** (1986). Thermal dependence of contractile properties of skeletal muscle from the lizard *Sceloporus occidentalis* with comments on methods for fitting and comparing force-velocity curves. *J. Exp. Biol.* **126,** 63–77.

**Marsh, R.L. and Bennett, A.F.** (1985). Thermal dependence of isotonic contractile properties of skeletal muscle and sprint performance of the lizard *Dipsosaurus dorsalis*. *J. Comp. Physiol. B* **155,** 541–551.

**Martin, L.B., Ghalambor, C.K. and Woods, H.A.** (2015). *Integrative organismal biology*. Hoboken, New Jersey: Wiley Blackwell.

**Mauro, A.A. and Ghalambor, C.K.** (2020). Trade-offs, pleiotropy, and shared molecular pathways: A unified view of constraints on adaptation. *Integr. Comp. Biol.* **60**, 332–347.

**Mayfield, D.L., Cresswell, A.G. and Lichtwark, G.A.** (2016). Effects of series elastic compliance on muscle force summation and the rate of force rise. *J. Exp. Biol.* **219,** 3261-3270.

**McGillivray, D.G., Garland Jr., T., Dlugosz, E.M., Chappell, M.A. and Syme, D.A.** (2009). Changes in efficiency and myosin expression in the small-muscle phenotype of mice selectively bred for high voluntary running activity. *J. Exp. Biol.* **212,** 977–985.

**Meek, T.H., Lonquich, B.P., Hannon, R.M. and Garland Jr., T.** (2009). Endurance capacity of mice selectively bred for high voluntary wheel running. *J. Exp. Biol.* **212,** 2908–2917.

**Mendez, J. and Keys, A.** (1960). Density and composition of mammalian muscle. *Metabolism* **9**, 184–188.

**Miles, M.C., Goller, F. and Fuxjager, M.J.** (2018). Physiological constraint on acrobatic courtship behavior underlies rapid sympatric speciation in bearded manakins. *eLife* **7,** e40630.

**Morris, C.R. and Askew, G.N.** (2010) The mechanical power output of the pectoralis muscle of cockatiel (Nymphicus hollandicus): The *in vivo* muscle length trajectory and activity patterns and their implications for power modulation. *J. Exp. Biol.* **213,** 2770-2780

**Nguyen, A., Balaban, J.P., Azizi, E., Talmadge, R.J. and Lappin, A.K.** (2020). Fatigue resistant jaw muscles facilitate long-lasting courtship behaviour in the southern alligator lizard (*Elgaria multicarinata)*. *Proc. R. Soc. B Biol. Sci.* **287,** 20201578.

**Pagala, M.K., Ravindran, K., Namba, T. and Grob, D.** (1998). Skeletal muscle fatigue and physical endurance of young and old mice. *Muscle Nerve* **21,** 1729–1739.

**Pasi, B.M. and Carrier, D.R.** (2003). Functional trade-offs in the limb muscles of dogs selected for running vs. fighting: Functional trade-offs of running vs. fighting. *J. Evol. Biol.* **16,** 324–332.

**Ranatunga, K.W.** (1984). The force-velocity relation of rat fast- and slow-twitch muscles examined at different temperatures. *J. Physiol.* **351,** 517–529.

**Renaud, J.M. & Kong, M.** (1991). The effects of isotonic contractions on the rate of fatigue development and the resting membrane potential in the sartorius muscle of the frog, *Rana pipiens*. *Can. J. Physiol. Pharmacol.* **69,** 1754–1759.

**Rhodes, J.S., Gammie, S.C. & Garland Jr., T.** (2005). Neurobiology of mice selected for high voluntary wheel-running activity. *Integr. Comp. Biol.* **45,** 438–455.

**Roach, G.C., Edke, M. and Griffin, T.M.** (2012). A novel mouse running wheel that senses individual limb forces: biomechanical validation and in vivo testing. *J. Appl. Physiol.* **113,** 627–635.

**Roberts, M.D., Ruegsegger, G.N., Brown, J.D. and Booth, F.W.** (2017). Mechanisms associated with physical activity behavior: Insights from rodent experiments. *Exerc. Sport Sci. Rev.* **45,** 217–222.

**Rome, L.C., Funke, R.P., Alexander, R.M., Lutz, G., Aldridge, H., Scott, F. and Freadman, M.** (1988). Why animals have different muscle fibre types. *Nature* **335,** 824–827.

**Santana, S.E.** (2016). Quantifying the effect of gape and morphology on bite force: Biomechanical modelling and *in vivo* measurements in bats. *Funct. Ecol.* **30,** 557–565.

**Saul, M.C., Majdak, P., Perez, S., Reilly, M., Garland Jr., T. and Rhodes, J.S.** (2017). High motivation for exercise is associated with altered chromatin regulators of monoamine receptor gene expression in the striatum of selectively bred mice. *Genes Brain Behav.* **16,** 328–341.

**Scales, J.A. and Butler, M.A.** (2016). Adaptive evolution in locomotor performance: How selective pressures and functional relationships produce diversity. *Evolution* **70**: 48–61.

**Schaeffer, P.J. and Lindstedt, S.L.** (2013). How animals move: Comparative lessons on animal locomotion. In: *Comprehensive Physiology.* Hoboken, NJ: John Wiley & Sons, Inc.

**Schiaffino, S. and Reggiani, C.** (2011). Fiber types in mammalian skeletal muscles. *Physiol. Rev.* **91,** 1447–1531.

**Spainhower, K.B., Cliffe, R.N., Metz, A.K., Barkett, E.M., Kiraly, P.M., Thomas, D.R., Kennedy, S.J., Avey-Arroyo, J.A. and Butcher, M.T.** (2018). Cheap labor: Myosin fiber type expression and enzyme activity in the forelimb musculature of sloths (*Pilosa: Xenarthra*). *J. Appl. Physiol.* **125,** 799–811.

**Swallow, J.G., Carter, P.A. and Garland Jr., T.** (1998). Artificial selection for increased wheel-running behavior in house mice. *Behav. Genet.* **28,** 227–237.

**Syme, D.A., Evashuk, K., Grintuch, B., Rezende, E.L. & Garland Jr., T.** (2005). Contractile abilities of normal and "mini" triceps surae muscles from mice (*Mus domesticus*) selectively bred for high voluntary wheel running. *J. Appl. Physiol.* **99,** 1308–1316.

**Talmadge, R.J., Acosta, W. & Garland, Jr., T.** (2014). Myosin heavy chain isoform expression in adult and juvenile mini-muscle mice bred for high-voluntary wheel running. *Mech. Dev.* **134,** 16–30.

**Thompson, M.A.** (2017). Physiological and biomechanical mechanisms of distance specific human running performance. *Integr. Comp. Biol.* **57,** 293–300.

**Toro, E., Herrel, A. and Irschick, D.** (2004). The evolution of jumping performance in Caribbean *Anolis* lizards: Solutions to biomechanical trade-offs. *Am. Nat.* **163**, 844–856.

**Vanhooydonck, B., James, R.S., Tallis, J., Aerts, P., Tadic, Z., Tolley, K.A., Measey, G.J. and Herrel, A.** (2014). Is the whole more than the sum of its parts? Evolutionary trade-offs between burst and sustained locomotion in lacertid lizards. *Proc. R. Soc. B Biol. Sci.* **281,** 20132677.

**Vanhooydonck, B., Van Damme, R. and Aerts, P.** (2001). Speed and stamina trade-off in lacertid lizards. *Evolution* **55,** 1040-1048.

**Williams, T.M., Dobson, G.P., Mathieu-Costello, O., Morsbach, D., Worley, M.B. and Phillips, J.A.** (1997). Skeletal muscle histology and biochemistry of an elite sprinter, the African cheetah. *J. Comp. Physiol.* **167,** 527–535.

**Wilson, R.S. and James, R.S.** (2004). Constraints on muscular performance: trade–offs between power output and fatigue resistance. *Proc. R. Soc. Lond. B Biol. Sci.* **271**, S222–S225

**Wilson, R.S., James, R.S. and Damme, R.V.** (2002). Trade-offs between speed and endurance. *J. Exp. Biol.* **205,** 1145-1152.

**Zhan, W.Z., Swallow, J.G., Garland, T., Proctor, D.N., Carter, P.A. & Sieck, G.C.** (1999). Effects of genetic selection and voluntary activity on the medial gastrocnemius muscle in house mice. *J. Appl. Physiol.* **87,** 2326–2333.

**Zhao, X., Yoshida, M., Brotto, L., Takeshima, H., Weisleder, N., Hirata, Y., Nosek, T.M., Ma, J. and Brotto, M.** (2005). Enhanced resistance to fatigue and altered calcium handling properties of sarcalumenin knockout mice. *Physiol. Genomics* **23,** 72–78.

# *Tables*

**Table 1.** Definitions of muscle dimensions and contractile properties of the triceps surae complex in HR mice.

| Abbreviations | Definition and Functional Significance |
|---|---|
| **$F_0$ (N)** | Peak isometric, tetanic force of the triceps surae complex |
| **Anatomical CSA ($cm^2$)** | Anatomical cross-sectional area of the triceps surae complex [((Triceps surae mass (g)'/1000)/1060)/ (Triceps surae length (mm)'/1000) *10000)] (Mendez & Keys, 1960) |
| **Stress ($N/cm^2$)** | Peak isometric, tetanic stress of the triceps surae complex [('$F_0$'/'Anatomical CSA')] (Askew & Marsh, 1997; Zhan *et al.*, 1999; Syme *et al.*, 2005; Holt *et al.*, 2016) |
| **$F_0$ Mass (N/g)** | Peak tetanic force of the triceps surae complex normalized to body mass [('$F_0$'/'Body Mass')] |
| **$TP_{tw}$ (ms)** | Time from muscle activation to peak twitch force (Marsh & Bennett, 1985, 1986; Bennett *et al.*, 1989; Askew & Marsh, 1997; Syme *et al.*, 2005) |
| **$TR_{50}$ (ms)** | Time from peak twitch force to 50% relaxation (Marsh & Bennett, 1985, 1986; Bennett *et al.*, 1989; Askew & Marsh, 1997; Syme *et al.*, 2005) |
| **$F/F_0$ (N)** | Active force of isotonic contractions divided by $F_0$ (0.1-0.9 $F_0$) (Marsh & Bennett, 1985, 1986; Bennett *et al.*, 1989; Askew & Marsh, 1997; Syme *et al.*, 2005; Holt *et al.*, 2016; Alcazar *et al.*, 2019) |
| **$V_{norm}$** | Shortening velocity in isotonic contractions (0.1-0.9 $F_0$) divided by muscle length (Marsh & Bennett, 1985, 1986; Bennett *et al.*, 1989; Askew & Marsh, 1997; Syme *et al.*, 2005; Holt *et al.*, 2016; Alcazar *et al.*, 2019) |
| **$V_{abs}$** | Absolute shortening velocity in isotonic contractions (Marsh & Bennett, 1985, 1986; Bennett *et al.*, 1989; Askew & Marsh, 1997; Syme *et al.*, 2005; Holt *et al.*, 2016; Alcazar *et al.*, 2019) |
| **$V_{normax}$ ($mm\ s^{-1}$)** | Maximal shortening velocity normalized by muscle length (Marsh & Bennett, 1985, 1986; Askew & Marsh, 1997; Zhan *et al.*, 1999; Syme *et al.*, 2005; Holt *et al.*, 2016; Alcazar *et al.*, 2019) |
| **$V_{max}$ ($mm\ s^{-1}$)** | Absolute maximal shortening velocity (Marsh & Bennett, 1985, 1986; Askew & Marsh, 1997; Zhan *et al.*, 1999; Syme *et al.*, 2005; Holt *et al.*, 2016; Alcazar *et al.*, 2019) |
| **$Endur_{0\text{-}90}$** | Linear fit (slope) of the first 90 isometric contractions of the triceps surae complex |

| | |
|---|---|
| **Sustained F (N)** | Sustained isometric force of the muscle after first 90 contractions of the fatigue protocol and after tetanic force stops declining |
| **Sustained F/ $F_0$ (N)** | Sustained isometric force normalized to peak tetanic force |

1006

1007

**Table 2.** Repeated-measures analyses for force-velocity measurements based on second-order polynomial fits for absolute velocity ($V_{abs}$) and normalized velocity ($V_{norm}$). For both dependent variables, the parameter estimates were negative for $F/F_0$, positive for $Z(F/F_0)^2$, and positive for age.

| $V_{abs}$ N=192 | F | d.f. | P | $V_{norm}$ N=184 | F | d.f. | P |
|---|---|---|---|---|---|---|---|
| **Group** | 102.44 | 4,180 | <0.0001 | | 56.48 | 4,172 | <0.0001 |
| **$F/F_0$** | 995.63 | 1,180 | <0.0001 | | 722.36 | 1,172 | <0.0001 |
| **$Z(F/F_0)^2$** | 39.67 | 1,180 | <0.0001 | | 24.18 | 1,172 | <0.0001 |
| **Age** | 85.85 | 1,180 | <0.0001 | | 101.71 | 1,172 | <0.0001 |
| **$F/F_0$ * Group** | 19.52 | 4,180 | <0.0001 | | 9.01 | 4,172 | <0.0001 |

| $V_{abs}$ | Least Squares Means | SE | | $V_{norm}$ | Least Squares Means | SE | |
|---|---|---|---|---|---|---|---|
| **L3 Mini** | 25.18 | 0.52 | | | 1.831 | 0.054 | |
| **L6 Mini** | 25.53 | 0.85 | | | 1.905 | 0.074 | |
| **L6** | 40.44 | 1.68 | | | 3.139 | 0.158 | |
| **L7** | 37.17 | 1.61 | | | 2.727 | 0.097 | |
| **L8** | 50.28 | 1.30 | | | 3.482 | 0.128 | |

**Table 3.** Pairwise Pearson correlations for Least Squares Means of force-velocity, endurance properties, and isometric contractile properties (N = 5), showing statistically significant correlations between $V_{normax}$ and $Endur_{0\text{-}90}$, $V_{normax}$ and Sustained $F/F_0$, and $Endur_{0\text{-}90}$ and Sustained $F/F_0$ (see Fig. 5).

| | | $V_{normax}$ | $Endur_{0\text{-}90}$ | Stress | $TP_{tw}$ | $TR_{50}$ | Sust. $F/F_0$ |
|---|---|---|---|---|---|---|---|
| $V_{normax}$ | Correlation | | -.993 | -.266 | .143 | -.148 | -.971 |
| | Sig. (2-tailed) | | .001 | .666 | .818 | .812 | 0.006 |
| $Endur_{0\text{-}90}$ | Correlation | | | .340 | -.040 | .111 | .961** |
| | Sig. (2-tailed) | | | .576 | .949 | .859 | 0.009 |
| Stress | Correlation | | | | .341 | .466 | 0.397 |
| | Sig. (2-tailed) | | | | .574 | .429 | 0.508 |
| $TP_{tw}$ | Correlation | | | | | -.261 | -0.146 |
| | Sig. (2-tailed) | | | | | .672 | 0.815 |
| $TR_{50}$ | Correlation | | | | | | 0.375 |
| | Sig. (2-tailed) | | | | | | 0.534 |

## *Fig. Legends*

Fig. 1. Fig. 1A: Least square means and standard errors of body mass for each line (L3 Mini, L6 Mini, L6, L7 and L8). Age was positively associated with body size and both L6 Mini and L7 mice were significantly lighter when compared with the other lines. Fig. 1B: Least square means and standard errors of triceps surae muscle length for each line. Neither age or body mass was associated with muscle length, and the lines did not differ significantly. Fig. 1C: Least square means and standard errors of triceps surae muscle mass for each line. Triceps surae muscle mass was positively associated with body mass, and mini-muscle mice (L3 Mini and L6 Mini) had significantly lighter muscles when compared with the other lines (L6, L7 and L8), with L7 having intermediate values. Fig. 1D: Least square means and standard errors of Anatomical CSA for each line. Mini-muscle mice (L3 Mini and L6 Mini) had significantly lower Anatomical CSA values when compared with the other lines. L3 Mini N=6, L6 Mini N=5, L6 N=6, L7 N=8, and L8 N=6 for all traits presented in this figure.

Fig. 2. Fig. 2A: Least square means and standard errors of Stress for each line (L3 Mini, L6 Mini, L6, L7 and L8). Neither age or body mass was associated with Stress and the lines did not differ significantly. Fig. 2B: Least square means and standard errors of $F_0$ Mass for each line. Mini-muscle mice (L3 Mini and L6 Mini) had significantly lower $F_0$ Mass values when compared with the other lines (L6, L7, and L8). Fig. 2C: Least square means and standard errors of $TP_{tw}$ for each line. Neither age or body mass was associated with $TP_{tw,}$ and the lines did not differ significantly. Fig. 2D: Least square means and standard errors of $TR_{50}$ for each line. Neither age or body mass was associated with $TR_{50,}$ and the lines did not differ significantly. L3

1043 Mini N=6, L6 Mini N=5, L6 N=6, L7 N=8, and L8 N=6 for all traits presented in this figure with
1044 the exception of $F_0$ Mass where L7 N=7.
1045
1046 Fig. 3. Fig. 3A: Representative force-velocity trace for L3 Mini, with ($F/F_0$) on the x-axis and
1047 absolute shortening velocity on the y-axis. The force-velocity points were curve-fitted using the
1048 second-order polynomials and maximal shortening velocity mm $s^{-1}$ estimates using this fit are
1049 visually rendered. Fig. 3B: Representative force-velocity trace for L6 Mini. Fig. 3C:
1050 Representative force-velocity trace for L6. Fig. 3D: Representative force-velocity trace for L7.
1051 Fig. 3E: Representative force-velocity trace for L8. Fig. 3F: Least square means and standard
1052 errors of $V_{max}$ $F_0$ Mass for each line based on second-order polynomials. $V_{max}$ was positively
1053 associated with age, and mini-muscle mice (L3 Mini and L6 Mini) had significantly lower $V_{max}$
1054 values when compared with the other lines (L6, L7 and L8). Of the normal-muscle lines, L8 had
1055 the highest $V_{max}$ value and L6 and L7 were intermediate. The repeated measured design of the
1056 force-velocity experiment meant there were a total of 192 total data points. Of these there were
1057 44 data points from 6 individuals in L3 Mini, 33 data points from 5 individuals in L6 Mini, 30
1058 data points from 4 individuals in L6, 53 data points from 7 individuals in L7, and 32 data points
1059 from 5 individuals in L8.
1060
1061 Fig. 4. Fig. 4A: Representative endurance trace wave profile for L3 Mini, with Contraction # on
1062 the x-axis and isometric force on the y-axis. The linear fit ($Endur_{0\text{-}90}$) of the decline in force over
1063 the first 90 tetanic contractions and the average sustained force (Sustained F) are visually
1064 rendered. Fig. 4B: Representative endurance trace wave profile for L6 Mini. Fig. 4C:
1065 Representative endurance trace wave profile for L6. Fig. 4D: Representative endurance trace

wave profile for L7. Fig. 4E: Representative endurance trace wave profile for L8. L8 mice all fatigued within the first 200 contractions. Fig. 4F: Least square means and standard errors of $Endur_{0\text{-}90}$ for each line. L3 Mini N=6, L6 Mini N=5, L6 N=6, L7 N=8, and L8 N=5. $Endur_{0\text{-}90}$ was positively associated with age, and mini-muscle mice (L3 Mini and L6 Mini) had significantly lower $Endur_{0\text{-}90}$ values when compared with the other lines (L6, L7 and L8), with L7 having intermediate $Endur_{0\text{-}90}$ values. Fig. 4F: Least square means and standard errors of Sustained $F/ F_0$ for each line. L3 Mini N=6, L6 Mini N=5, L6 N=5, L7 N=6, and L8 N=3 Mini-muscle mice (L3 Mini and L6 Mini) had significantly lower Sustained $F/ F_0$ values when compared with the other lines.

Fig. 5. Fig. 5A: Scatterplot of least squares means and standard errors for $V_{normax}$ (normalized maximal shortening velocity) and $Endur_{0\text{-}90}$ (linear slope of the first 90 contractions). $V_{normax}$ and $Endur_{0\text{-}90}$ have a negative relationship. Mini-muscle mice (L3 Mini and L6 Mini) have the highest endurance ($Endur_{0\text{-}90}$) but slowest muscles ($V_{normax}$), L6 and L8 have the lowest endurance but fastest muscles, and L7 is intermediate. Fig. 5B: Scatterplot of least squares means and standard errors for $V_{normax}$ (normalized maximal shortening velocity) and Sustained $F/F_0$ (normalized force that can be sustained). $V_{normax}$ and Sustained $F/F_0$ have a negative relationship. Mini-muscle mice (L3 Mini and L6 Mini) have the highest sustained force (Sust. $F/F_0$) but slowest muscles ($V_{normax}$), L8 has the lowest sustained force but the highest $V_{normax}$. Fig. 5C: Scatterplot of least squares means and standard errors for Sustained $F/F_0$ and $Endur_{0\text{-}90}$. Sustained $F/F_0$ and $Endur_{0\text{-}90}$ have a positive relationship as would be expected given that they are both metrics of muscle endurance. N values are as for Fig. 3 and Fig. 4.

1089 Figure 1

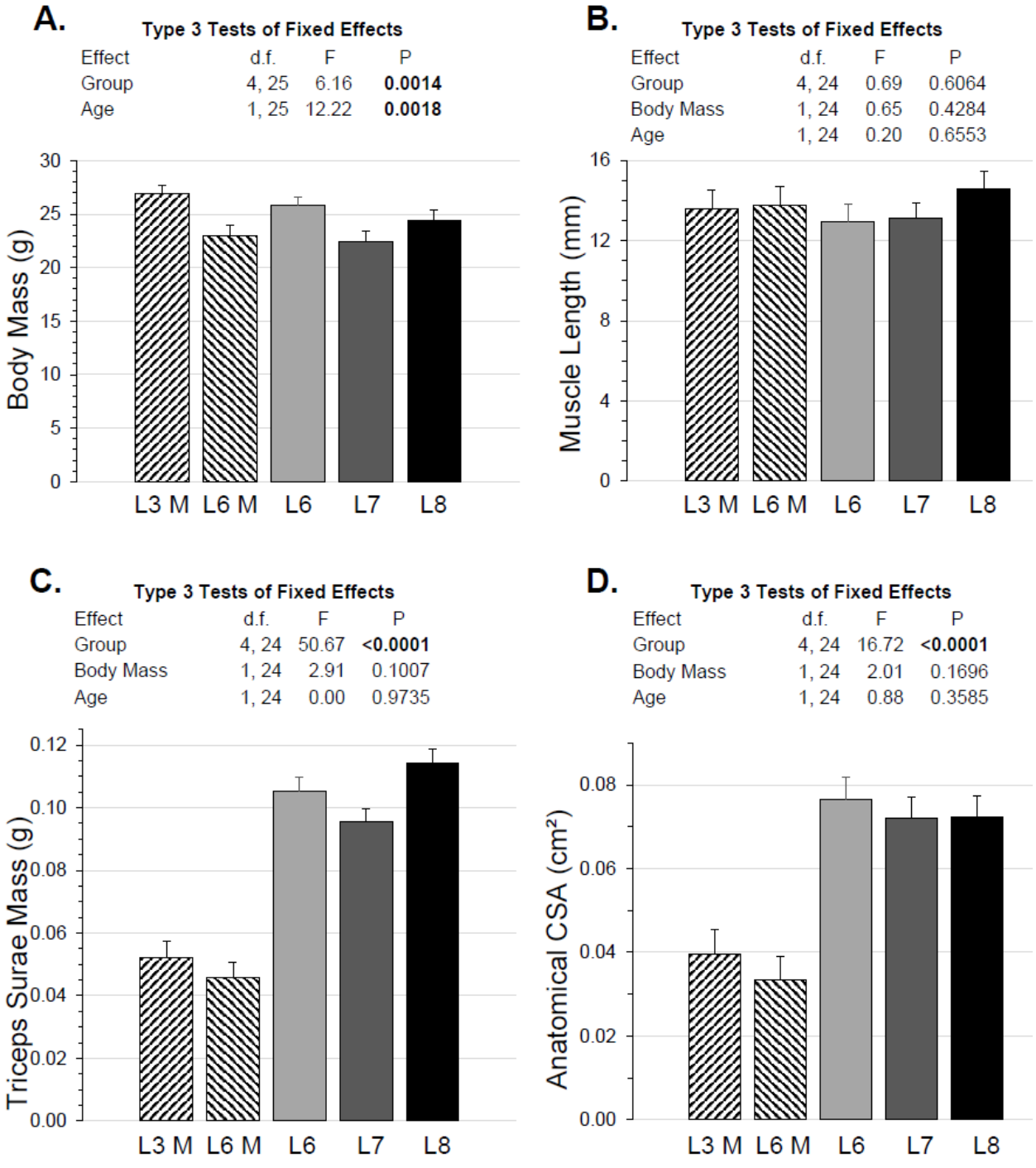


1090

1091

1092 Figure 2

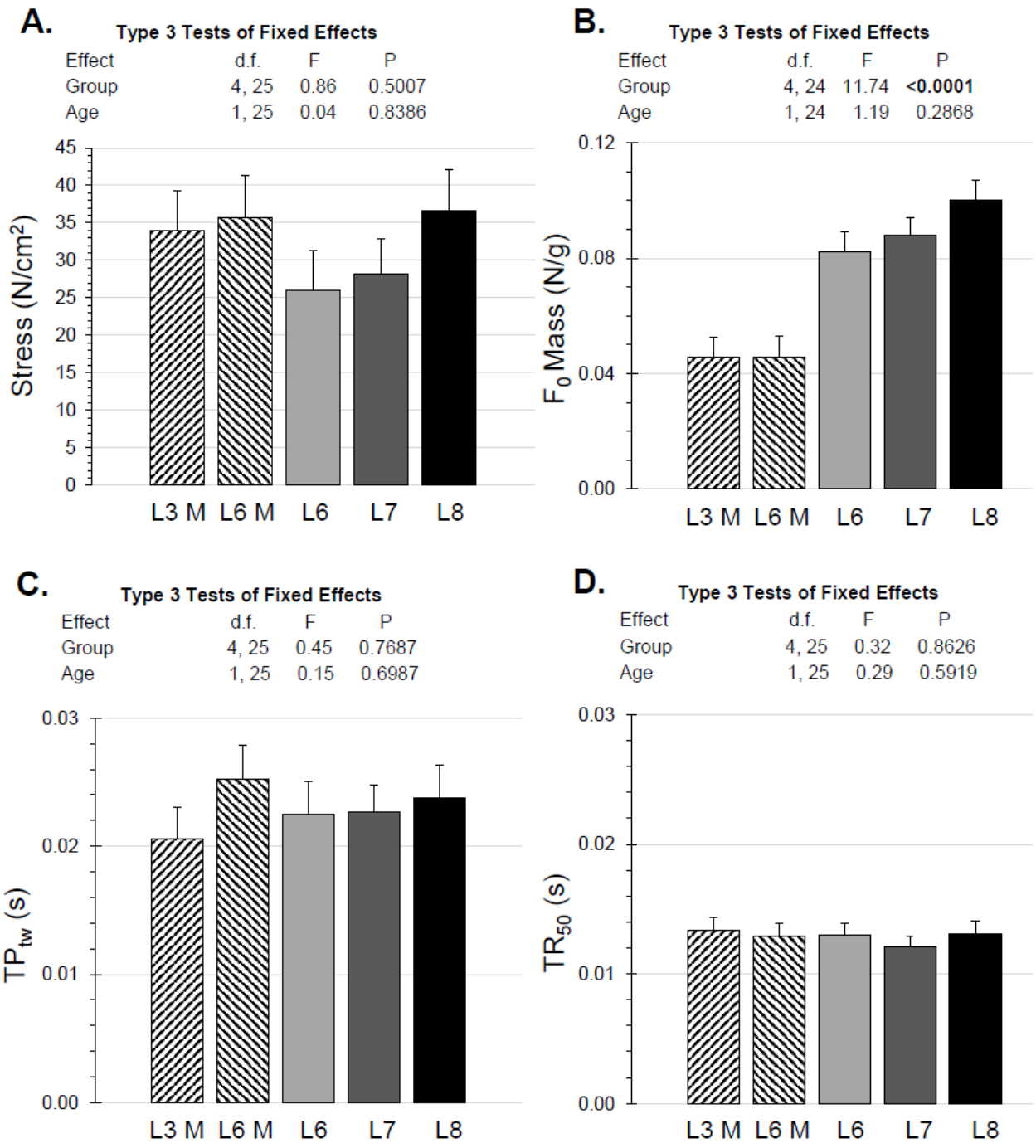


1093

1094

1095 Figure 3

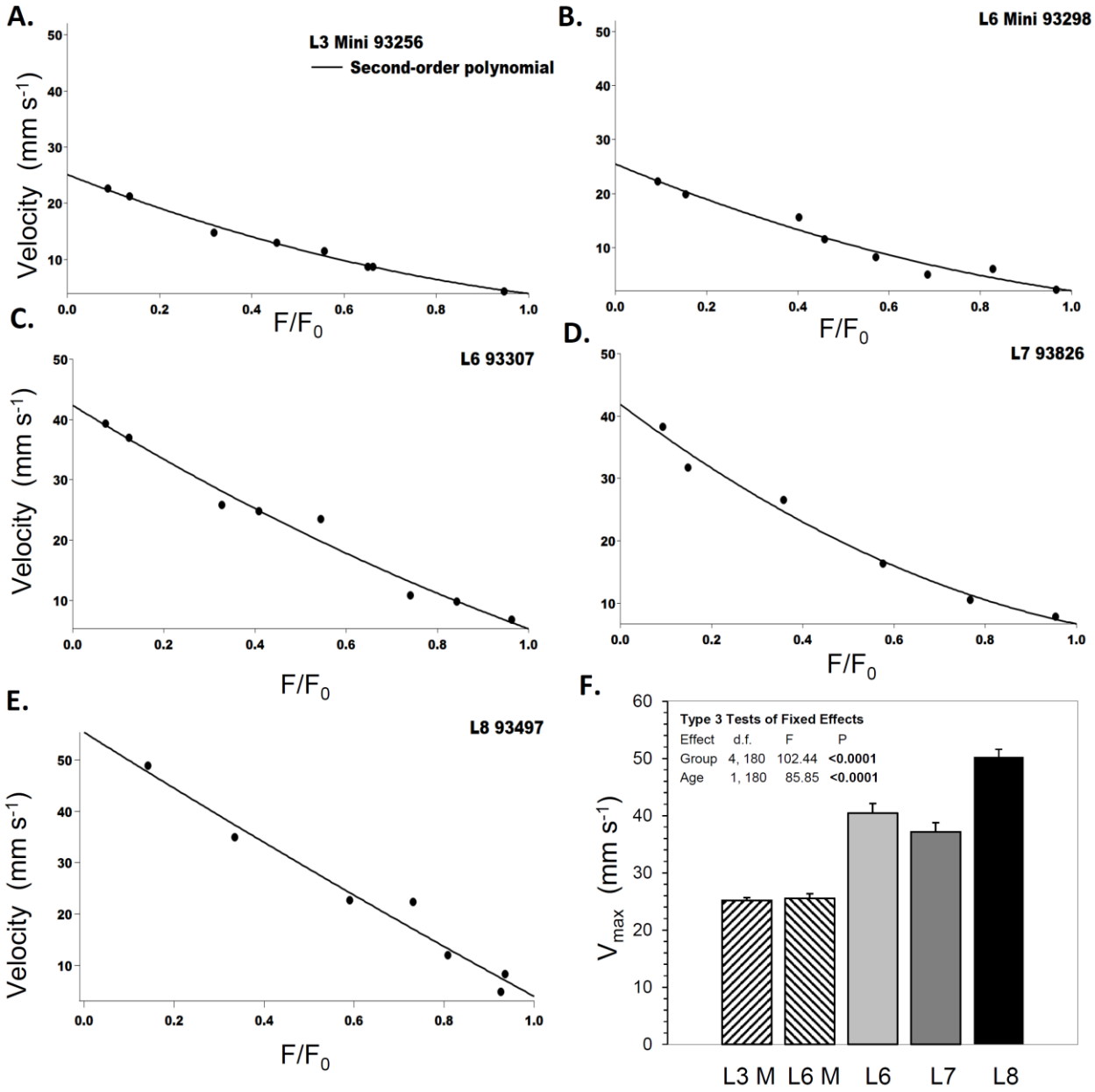


1096

1097

1098 Figure 4

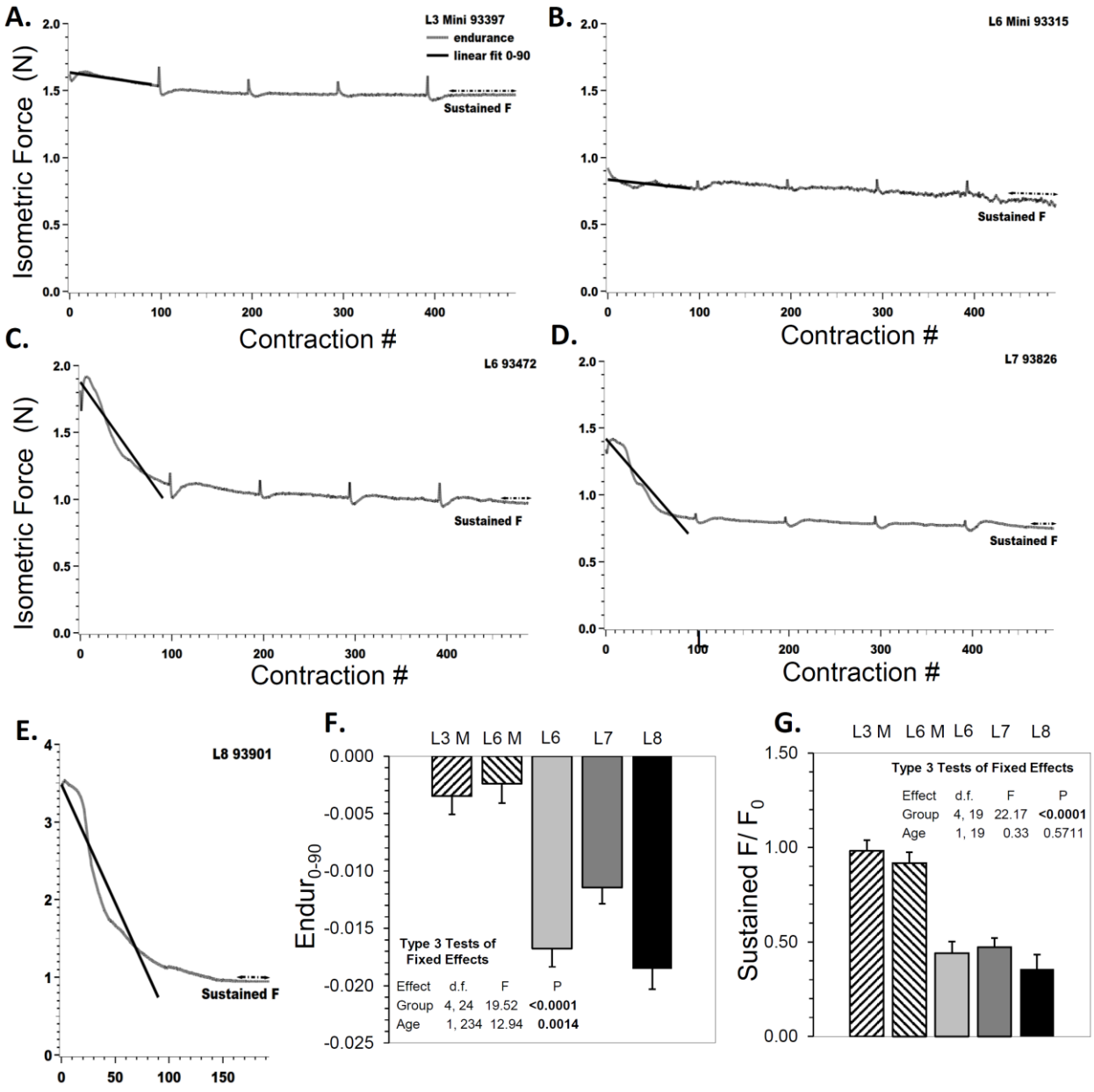


1099

1100

1101 Figure 5

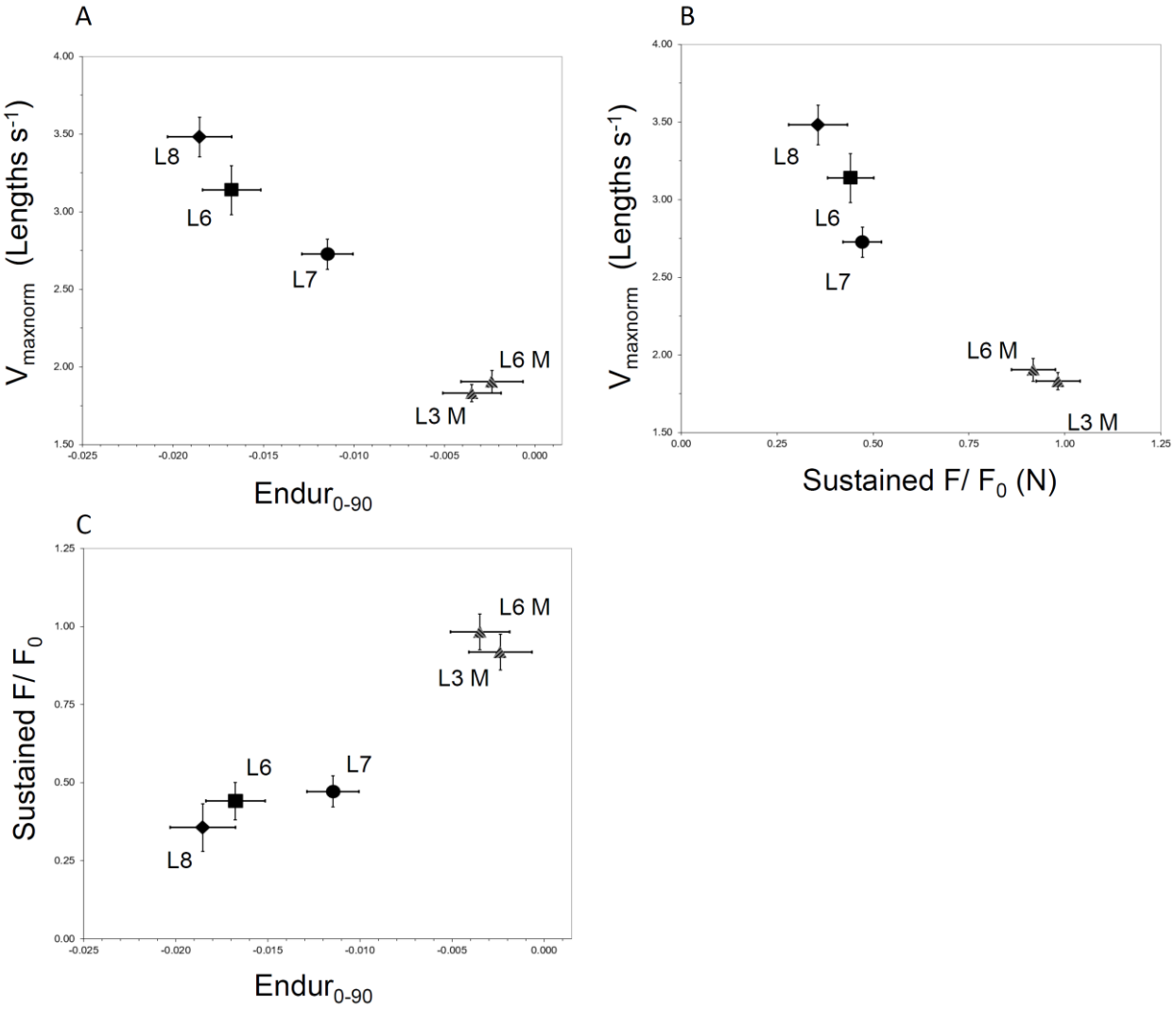


1102

1103

1104